Final Report
Investigation of the
Transport of Solar Ions Through the Earth's Magnetosphere

Grant NAGW-4177 and Contract NASW-97012

August 1, 2000

(period of performance ending July 31, 2000)

The objective of this study has been to infer, by statistical means, the most probable mode of entry of solar wind plasma into Earth's magnetotail, using a particular set of archived data from the Lockheed Plasma Composition Experiment on the International Sun-Earth Explorer One (ISEE-1) satellite, jointly sponsored by the National Aeronautics and Space Administration (NASA) and the European Space Agency (ESA) in the 1970's and 80's. Despite their considerable age, the Lockheed ISEE-1 data are still, at the time of this report, the only substantial ion composition data in the sub-keV to keV energy range available from the magnetotail beyond 9 R_E, because of various technical problems with ion mass spectrometers on later missions, and are therefore a unique source of information about the mixing of solar and terrestrial origin plasmas in the tail, within the ISEE-1 apogee of almost 23 R_E. The entire set of archived data used in this study, covering the 4.5 years of operation of the instrument and comprising not only tail measurements but also data from the inner magnetosphere as well as data from outside the magnetopause, is now available to the public via the WorldWideWeb at the address:

http://cis.spasci.com/ISEE_ions

The fundamental assumption of this and other studies of magnetosphere ion composition is that He^{++} and O^+ ions are virtually certain "tags" of solar and terrestrial origins, respectively. This is an assumption with strong theoretical basis and it is corroborated by observational evidence, including the often substantial differences between the velocity distribution functions of those two species. The H^+ ions can have a dual origin, in principle, but the close resemblance in the ISEE-1 data between the dynamics of H^+ and He^{++} ions indicates a predominantly solar origin of the H^+ ions in the tail, at least. By the same token, the usually minor He^+ ions are probably almost entirely of terrestrial origin, because of their similarity to the O^+ ions.

O.W. Lennartsson
Principal Investigator

The results of this study are described in the following sections:

Statistical Properties of Tail Ion Flows

O.W. Lennartsson

Lockheed Martin Space Systems /Advanced Technology Center
Palo Alto, California

August 2000

Excerpt from a manuscript being prepared for submission to *Journal of Geophysical Research*

1. Introduction

When originally proposed, this study was motivated in large part by the prospect that the solar wind plasma enters Earth's magnetotail along its flanks, specifically along some kind of slot between the high-latitude plasma mantle (tail lobe magnetopause boundary layer [e.g. *Rosenbauer et al.*, 1975]) and the LLBL (low latitude magnetopause boundary layer [e.g. *Eastman et al.*, 1976]). Some evidence in that direction had emerged in previous studies of the ISEE-1 ion composition data [*Lennartsson*, 1992], and the implications were that the plasma sheet is being populated from the magnetosheath along its tailward extent, beginning near Earth, contrary to the traditional image of earthward flow of magnetosheath plasma from a distant tail reconnection site or "neutral line" [e.g. *Cowley*, 1980]. Furthermore, it had been revealed by the ISEE-1 data on H^+ and He^{++} ions [*Lennartsson*, 1992, and references therein], and later corroborated by positive ion data without mass resolution from other missions [e.g. *Fujimoto et al.*, 1997], that the solar wind has ready access to Earth's plasma sheet even during extended periods of northward IMF (interplanetary magnetic field) B_z, which is when standard geomagnetic indices are usually at their lowest levels and the magnetosphere would be expected to be essentially "closed" in terms of magnetic merging/reconnection. However, it has proved difficult to find unambiguous evidence of the entry process itself, in terms of the associated inward ion flows, as discussed in Appendix I, the main reason being that the plasma sheet varies rapidly and greatly in spatial extent [c.f. *Hones et al.*, 1971]. This report illustrates and tabulates new results from the most extensive statistical study to date of the ISEE-1 ion composition data with regard to ion bulk flows, placing the emphasis on three species, namely H^+, He^{++} and O^+ ions.

To appreciate the results to follow it is helpful to consider Figure 1. This is a tailward projection of constant magnetic latitude at ionospheric altitude (100 km alt), using field line tracing in the *Tsyganenko* [1987] average magnetic field model for Kp = 2. For simplicity, a time has been chosen when Earth's dipole is perpendicular to the Sun-Earth line and the tail therefore symmetrical in the GSM north-south direction. The most important aspect of this figure is that the model magnetic filed lines near the dawn and dusk flanks of the tail are *closed* through the equatorial plane, even those that have their ionospheric foot point as far poleward as ±77° latitude (those at ±78° and further poleward do project tailward at all local times). This means that the auroral zones are probably on closed field lines for the most part, at least over some wide local-time ranges that project into the tail flanks. Because of the tailward bending of the field lines, their foot points may be on the dayside. Specifically, the field lines from ±77° latitude that barely touch the GSM $x = -15$ R_E plane at $z = 0$ and $y \sim \pm 23$ R_E start at magnetic local times of 15:12 and 08:48 MLT, respectively.

If we imagine that the ionospheric plasma drift at ~ ±77° latitude (~most poleward portion of auroral zones) is generally directed from the dayside toward local midnight, then there must be a corresponding *inward* **E×B** drift in the tail, away from the flanks toward the tail center, as indicated by the outer set of arrows in Figure 1. Likewise, if we consider sunward return flow at lower latitude in the ionosphere, then we are dealing with *outward* **E×B** drift in the tail, away from the tail center, as indicated by the inner set of arrows in Figure 1. These two sets of drifts can be naturally connected near local midnight by equatorward convection. For symmetry (and other) reasons, the drifts in the equatorial plane must be perpendicular to the plane of this figure, specifically in the tailward direction in the outer flanks, that is in the LLBL, and sunward further in [*Lennartsson*, 1992].

The main objective of this study has been to search for evidence of this kind of cross-tail plasma convection, a kind of convection that would materially connect the plasma sheet with the LLBL, which is known to be dominated by solar origin plasma [*Eastman et al.*, 1976; *Mitchell et al.*, 1987], and perhaps with the magnetosheath, as well, along "slots" between the LLBL and the plasma mantle. The technical approach has been dictated in large measure by the problem of defining "position" within a plasma population whose "dimensions" are continually varying.

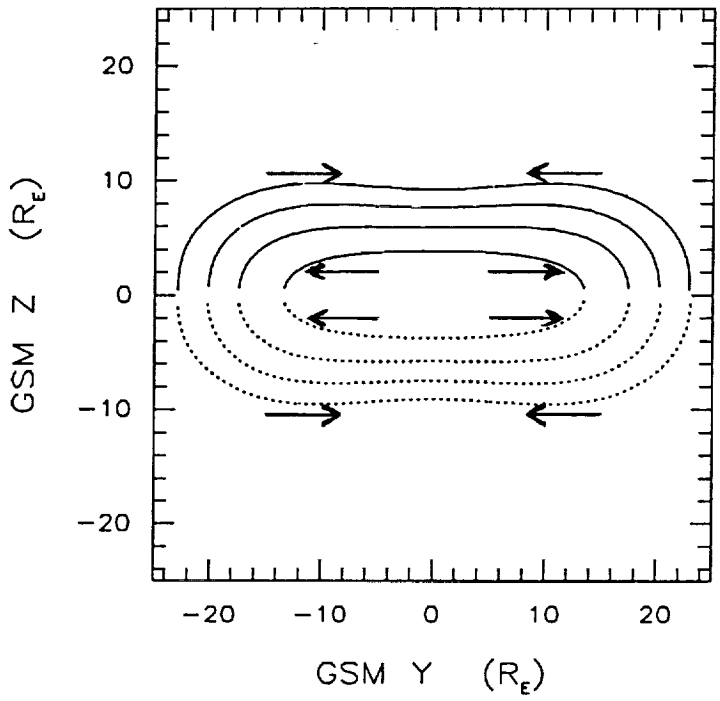

Figure 1. Projections of (partial) geomagnetic latitude circles ±71°, ±73°, ±75° and ±77° (outward is poleward) onto the GSM (geocentric solar-magnetic) y-z plane at $x = -15$ R_E along magnetic field lines in the *Tsyganenko* [1987] model when dipole is perpendicular to Sun-Earth line (e.g. ~10:40 UT on 20 March 1980) and Kp = 2. The respective equatorial intersections ($z = 0$), counted outward, correspond to field lines beginning at magnetic local times (MLT) that are ±7.1, ±5.8, ±4.8 and ±3.2 hours from local noon (same for northern and southern latitudes in this case). Arrows indicate expected direction of plasma convection (see text).

A brief note on the GSM and GSE coordinate systems is appropriate here, since they are used extensively below. Both systems have their origin at the center of Earth and the x-axis pointing at the Sun, but while the GSE (geocentric solar ecliptic) has its z-axis fixed and pointing at the ecliptic North, the GSM (geocentric solar magnetic) has a pivoting z-axis so as to include Earth's magnetic dipole within the x-z-plane. The y-axis completes each system by pointing in a dawnward direction.

2. Technical Approach

The ISEE-1 Plasma Composition Experiment is described in *Shelley et al.* [1978], and further details about the instrument and its performance in flight are provided in an extensive Data User's guide posted at the web site *http://cis.spasci.com/ISEE_ions*. Only a few instrumental aspects need mentioning here, along with some basic features of the data format.

(1) The full energy range is 0 eV/*e* (or s/c potential) to 18 keV/*e*, but the data presented here cover essentially 0.1 to 16 keV/*e*, unless stated otherwise in some special case.

(2) While the instrument was built with two sensor heads, all data presented here are from one of those, the one with its mass resolving detector viewing 5° below the s/c spin plane, which means about 5° below the solar ecliptic plane. Due to a 3000 V preacceleration of incoming ions, the angular acceptance perpendicular to the ecliptic plane varies with ion energy from ~ ±20° at low energy to ±5° at the highest energies. This means, in particular, that the ecliptic plane is well within the field of view at energies below 10 keV/*e*. The (instantaneous) angular acceptance in the spin direction is ±5°.

(3) In addition to the mass resolving detector, which is electronically cycled through different mass per charge (*M/Q*), usually at each energy step, the detector head also has a positive-ion sensor, viewing above or along the ecliptic, which provides continuous measurements at the rate of the energy (*E/Q*) cycle (typically 1-3 min).

(4) At the lower s/c telemetry rate normally used (~80% of the time) the angular resolution in the spin direction is ~30° (s/c spin period is 3 sec). This has been the standard angular width for binning here.

(5) The instrument was operated in many different cycling modes, each designed to emphasize some particular sampling sequence of the ions' velocity space, often including a special "cold plasma" sampling with the RPA portion of the instrument (at $E/Q < 100$ eV/*e*). While most modes concentrated on 4-6 isolated *M/Q* settings, plus detector background samplings, they usually included separate and complete mass spectral scans at a subset of the 32 energies. As a consequence, the instrument cycles ranged in length from a few minutes to as much as 20 min, with a "typical" cycle taking about 15 min. These variable-length cycles define the basic but variable *time resolution* of the archived ion composition data.

(6) Assuming that H^+ ions are the dominant component (usually the case), the positive-ion sensor does provide a complementary set of measurements at a time resolution of 1-3 min. These are referred to as "total ion" measurements below.

2.1. Spatial Constraints on Tail Flow Study

The apogee of the ISEE-1 satellite, at GSM R slightly below 23 R_E, forms the outer boundary for this study. For the inner boundary, two conditions have been used:

$$\text{GSM } R > 10\ R_E \quad \text{and} \quad \text{GSM } x < -5\ R_E$$

2.2. Exclusion of Magnetosheath

Automatic screening against magnetosheath (and solar wind) encounters has been based on both count rate levels and velocity moments and both composition data (H^+ and He^{++}) and "total ion" data.

Specifically, all data from a given instrument cycle have been discarded if at any time during that cycle the count rate exceeded a level that triggered the automatic gain reduction, a condition known to occur in the magnetosheath on a regular basis. In addition, data were rejected when the H^+ or (peak) "positive ion" density exceeded 10 cm^{-3}, or the He^{++} density 0.5 cm^{-3}, in combination with > 50 km s^{-1} tailward flow.

2.3. Latitudinal Separation of Plasma Sheet Flow Data

Being that the tail magnetic field and the plasma sheet are normally in diamagnetic balance [e.g. *Fairfield et al.*, 1981], it follows that the local ratio between total ion gyrational energy density and the magnetic energy density, the beta value, is a measure of the relative position between the central plasma sheet and a tail lobe. It is only a crude such measure, but it is far superior to any measure using fixed spatial coordinates, since the spatial thickness of the plasma sheet is strongly variable [e.g. *Hones et al.*, 1971]. Using beta is further justified by the fact that it does order the flow data to a considerable degree. The beta is defined here by summing the four major ionic contributions (H^+, He^{++}, He^+ and O^+) as measured over the 0.1-16 keV/*e* range, including, for simplicity, the small (≤few %) drift energy as well:

$$\beta = \{\Sigma_i \, 2^{-1} \, n_i \, m_i \langle v_{i\perp}{}^2 \rangle\} \, 2\mu_0 \, B^{-2}$$

where ⟨⟩ indicates mean of distribution and B is the magnetic field strength measured by the ISEE-1 magnetometer [*Russell*, 1978] and averaged over the entire ion measurement cycle (e.g. ~15 min). The "latitude" of the measurements is defined by a combination of beta and the magnetic field elevation angle relative to the ISEE-1 spin plane, i.e. essentially the ecliptic plane, in the following manner:

"High" and "intermediate" plasma sheet latitudes are used for most of the data displays and both have the magnetic field vector within ±9° of the spin plane during a given ion measurement cycle. This ensures that at least one of the two field-aligned directions of motion is sampled at all ion energies (see instrumental point #2 above). In terms of "earthward" and "tailward", this definition has proved to yield a fairly uniform statistical sampling of both field directions. Thus given that (in GSE coordinates)

$$|B_z| << (B_x{}^2 + B_y{}^2)^{1/2} \qquad (2.3.1)$$

the subdivision between these two latitudes is by beta:

$$\text{High latitude:} \quad \beta < 0.1 \qquad (2.3.1a)$$

$$\text{Intermediate:} \quad \beta > 0.1 \qquad (2.3.1b)$$

"Low" or "near-equatorial" latitude, used in only a few cases, is defined by $\beta > 0.1$ and

$$|B_z| > (B_x{}^2 + B_y{}^2)^{1/2} \qquad (2.3.2)$$

2.4. Separation of Flow Data by Solar Wind Conditions

Information on the concurrent solar wind conditions has been extracted from a tape copy of the National Space Science Data Center's (NSSDC) electronic OMNI file [*Couzens and King*, 1986]. The information is in the form of hourly Universal Time averages of the plasma and magnetic field (IMF) parameters and is available for about 80% of the ISEE-1 data. For this study the use of OMNI parameters has been limited to the GSM B_z component of the IMF to identify and separate ISEE-1 data taken during "north-IMF" and "south-IMF" conditions. Those two conditions have each been defined by two

consecutive hourly values $B_z(h\text{-}1)$ and $B_z(h)$, where h and h-1 are the current and preceding UT hours, respectively:

$$\text{IMF } B_z \geq 0: \quad B_z(h\text{-}1) \text{ and } B_z(h) \text{ both} \geq 0 \qquad (2.4.1a)$$

$$\text{IMF } B_z < 0: \quad B_z(h\text{-}1) \text{ and } B_z(h) \text{ both} < 0 \qquad (2.4.1b)$$

Requiring that two hourly IMF B_z values have the same sign reduces the number of "good" ISEE-1 samplings by an additional 20%, which means that the IMF-sorted data comprise about 65% of the initial set.

3. Statistical Results

3.1. High and Intermediate Latitudes

This study has dealt with two physically related but observationally different issues, namely (1) the average *direction* (in degrees) of ion bulk flows and (2) the average *density* (in $m^{-2}\,s^{-1}$) of flows in a given direction. The first issue, unlike the second one, is meaningful only to the extent that a velocity measurement is *significant* in terms of counting statistics, and this inevitably leads to a sampling bias against both low speeds and low count rates. Hence, the results on flow angles apply primarily to enhanced flow speeds for each ion species, and the results for different species are based on somewhat different statistical populations. In particular, average flow angles of He^{++} ions are based on far fewer samplings than those of the more abundant H^+ ions and tend to favor times of enhanced percentage of He^{++} ions. The "significance" of each velocity measurement is determined from the propagated standard deviations of Poisson counts listed in the archival ISEE-1 files and is defined by

$$|v_x| > 2.5\ \sigma(v_x) \quad \text{or} \quad |v_y| > 2.5\ \sigma(v_y)$$

that is, at least one of the two velocity components must have a magnitude more than 2.5 times its own standard deviation.

3.1.1. RESULTS WITH SIGNIFICANT DRIFT VELOCITIES

Figures 2, 3 and 4 show the frequency of occurrence of "adjusted" flow angles in the ecliptic plane at "high" ($\beta < 0.1$) and "intermediate" ($\beta > 0.1$) latitudes for H^+, He^{++} and O^+ ions respectively. The angles are adjusted in the sense that 0° and 180° are aligned with the local GSE x-y projection of **B**. Because of 2.3.1 above, this means essentially along the magnetic field vector itself. These angular distributions have not been sorted by solar wind conditions.

In order to agree with the drift arrows in Figure 1 (**E**×**B** drift), in the average sense, the preferred flow angles in these figures need to cluster at <180° in the top left and bottom right panels and at >180° in the top right and bottom left panels. There are indeed trends in those directions, but the scatter is considerable. Similar trends in ISEE-1 and ISEE-2 ion flow data have previously been reported specifically for intense tailward "streams" of O^+ ions by *Orsini et al.* [1990].

Table 1 quantifies these results in terms of net eastward drift velocity perpendicular to **B**, and it also separates the samplings by IMF B_z. The errors indicated here and in following tables reflect the standard deviations of the calculated means. These are caused by the scatter of samplings and have little or no relation to the precision of each velocity measurement. Values with parantheses refer to points at GSM $|y| > 10\ R_E$, values without include all GSM y, as do Figures 2, 3 and 4.

Table 2 lists the corresponding ion number densities (all GSM y). As can be seen, the He^{++}/H^+ ratios are somewhat elevated above normal values, especially at $\beta < 0.1$ (~10%), due to the requirement that all velocity measurements be significant.

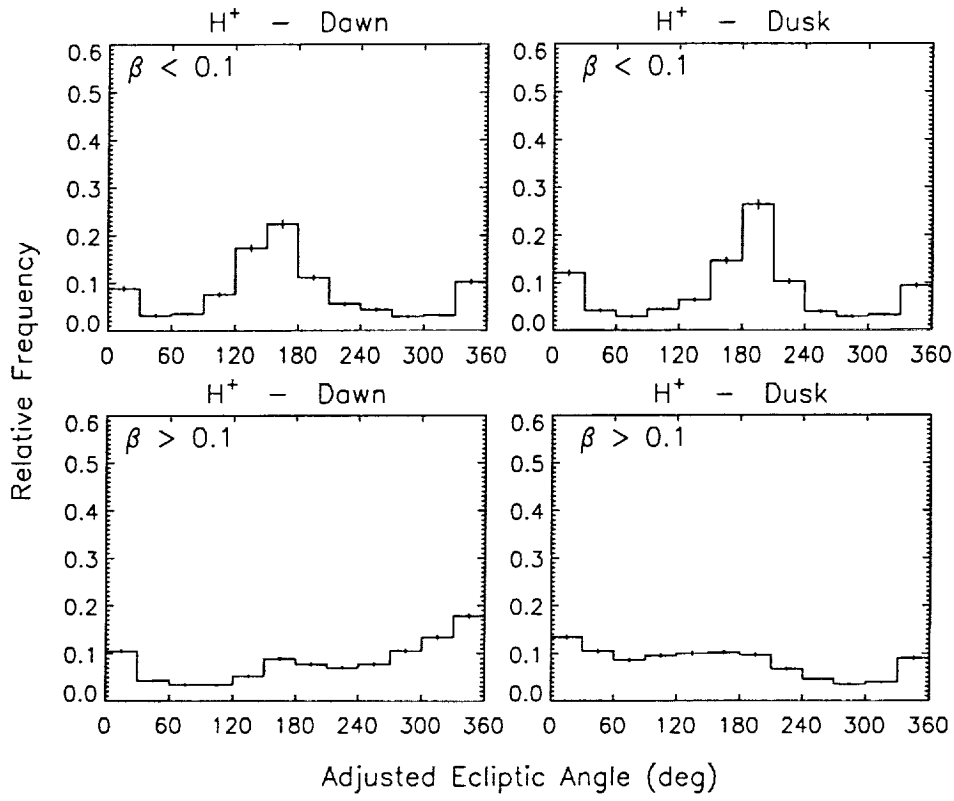

Figure 2. Relative rates of occurrence of H^+ drift angle in GSE (geocentric solar-ecliptic) x-y plane (~instrument field of view), binned in 30° intervals, in the (left) dawn and (right) dusk halves of the plasma sheet at (top) high and (bottom) intermediate latitude, where "latitude" is defined by the measured ion beta value (0.1-16 keV/e). The drift angle is adjusted by the local ecliptic angle of the magnetic field so that 180° means tailward parallel to the field line. Error bars indicate ± one standard deviation ($n^{1/2}$ $[\Sigma n]^{-1}$). Data span ca 4.5 years of observations but are limited to (1) statistically significant (> 2.5σ) velocity measurements and (2) latitudes where tail $|B_z| << (B_x^2+B_y^2)^{1/2}$ (see text).

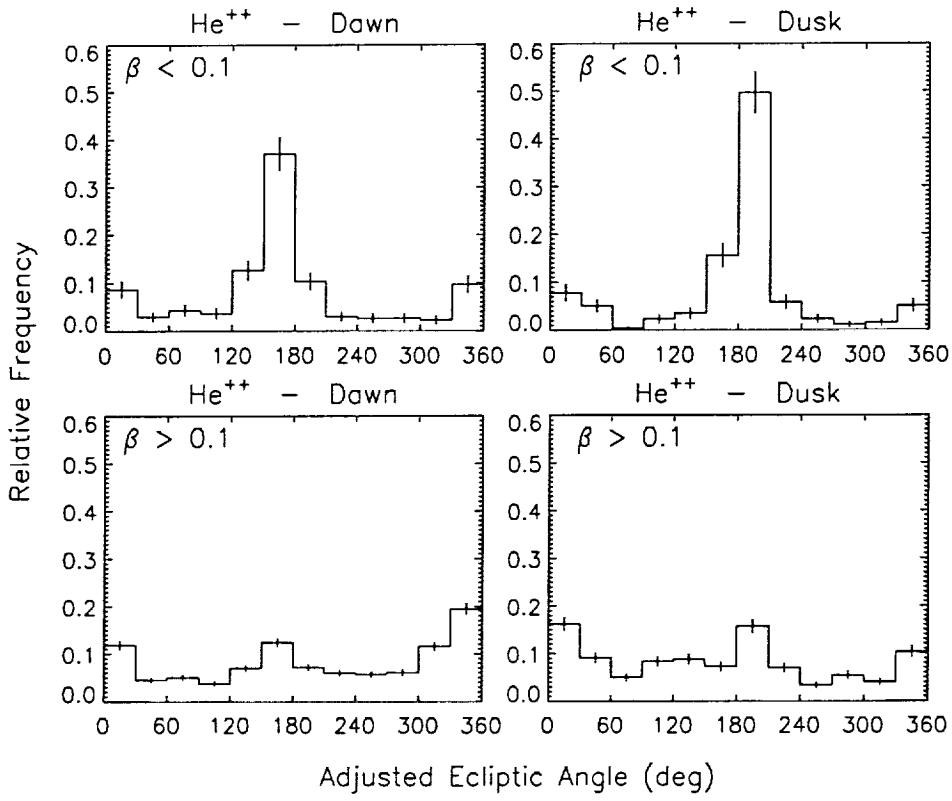

Figure 3. Same as Figure 2 but for He^{++} ions.

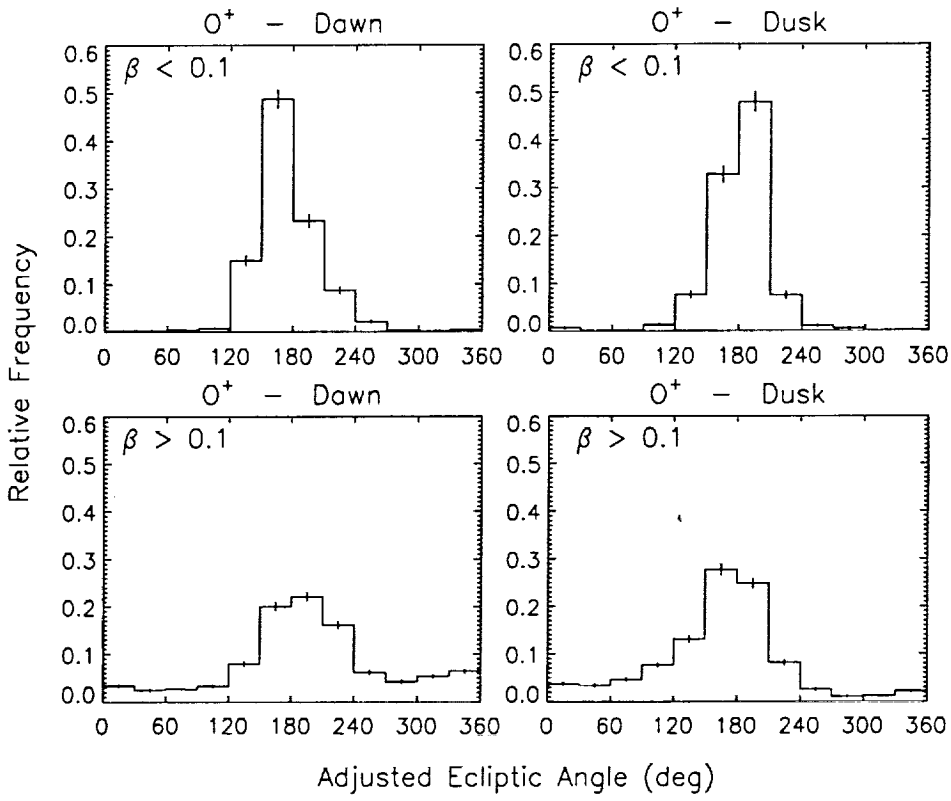

Figure 4. Same as Figure 2 but for O^+ ions.

Table 1. Net Eastward ($-y$) Component (km s^{-1}) of Significant ($> 2.5\ \sigma$) Velocities

	IMF $B_z \geq 0$					
	Dawn			Dusk		
	H^+	He^{++}	O^+	H^+	He^{++}	O^+
$\beta < 0.1$:	-7 ± 1	-7 ± 6	-2 ± 1	4 ± 1	-2 ± 8	4 ± 2
	(-16 ± 6)	(-38 ± 19)	(-3 ± 6)	(13 ± 3)	(7 ± 15)	(6 ± 2)
$\beta > 0.1$:	8 ± 1	8 ± 2	2 ± 1	-6 ± 1	-13 ± 3	-7 ± 1
	(6 ± 1)	(2 ± 3)	(-3 ± 2)	(-4 ± 1)	(-10 ± 4)	(-5 ± 2)
	IMF $B_z < 0$					
	Dawn			Dusk		
	H^+	He^{++}	O^+	H^+	He^{++}	O^+
$\beta < 0.1$:	-16 ± 1	-18 ± 5	-6 ± 1	1 ± 2	5 ± 5	3 ± 1
	(-17 ± 2)	(-18 ± 5)	(-4 ± 2)	(13 ± 2)	(11 ± 5)	(7 ± 2)
$\beta > 0.1$:	15 ± 1	12 ± 4	14 ± 1	-14 ± 1	-25 ± 6	-12 ± 1
	(14 ± 2)	(13 ± 5)	(13 ± 2)	(-19 ± 1)	(-15 ± 8)	(-16 ± 2)

Table 2. Density (cm^{-3}) of Ions at Times of Significant Drift Velocity Measurement

	IMF $B_z \geq 0$					
	Dawn			Dusk		
	H^+	He^{++}	O^+	H^+	He^{++}	O^+
$\beta < 0.1$:	.110 ± .007	.009 ± .001	.056 ± .004	.15 ± .01	.019 ± .002	.024 ± .002
$\beta > 0.1$:	.51 ± .01	.028 ± .001	.067 ± .004	.44 ± .01	.022 ± .002	.073 ± .006

	IMF $B_z < 0$					
	Dawn			Dusk		
	H^+	He^{++}	O^+	H^+	He^{++}	O^+
$\beta < 0.1$:	.092 ± .004	.012 ± .001	.059 ± .004	.108 ± .006	.015 ± .002	.051 ± .004
$\beta > 0.1$:	.36 ± .01	.020 ± .001	.065 ± .004	.27 ± .01	.017 ± .002	.066 ± .005

Table 3. H^+ Drift Speed (> 2.5 σ) Along Given Direction (± 30°) in km s^{-1}

	IMF $B_z \geq 0$							
	Dawn				Dusk			
	$+x$	$+y$	$-x$	$-y$	$+x$	$+y$	$-x$	$-y$
$\beta < 0.1$:	185 ±14	49 ± 4	59 ± 3	51 ± 7	195 ±17	45 ± 8	75 ± 3	49 ± 6
$\beta > 0.1$:	79 ± 4	40 ± 4	52 ± 3	44 ± 2	86 ± 6	39 ± 2	64 ± 3	39 ± 3
	IMF $B_z < 0$							
	Dawn				Dusk			
	$+x$	$+y$	$-x$	$-y$	$+x$	$+y$	$-x$	$-y$
$\beta < 0.1$:	232 ±21	77 ± 6	84 ± 3	65 ± 8	291 ±22	87 ±12	99 ± 3	77 ± 6
$\beta > 0.1$:	125 ± 7	67 ± 7	84 ± 5	56 ± 3	132 ±10	60 ± 3	79 ± 5	61 ± 5

Table 3 shows average H^+ drift speeds in 60° bins (paired bins) centered on the major axes. These are in fact somewhat larger than true averages (by a factor of 2-3), again due to the requirement that measurements be significant (H^+ has the best counting statistics). The largest *speeds* tend to occur earthward along the magnetic field (~ $+x$) at $\beta < 0.1$, a fact that will be elaborated on below.

Table 4 shows the corresponding H^+ mean energies, which are much larger than the respective drift energies (by factors >10). In this table, and in others to follow, some bins have been combined when there is no statistically significant difference between averages (dawn and dusk and $+y$ and $-y$ here).

Table 5 shows the corresponding parallel-to-perpendicular H^+ energy ("temperature") ratios. For the most part these indicate near-isotropy, as do the statistically less precise He^{++} ratios (not shown). By comparison, the O^+ ions have a substantially field-aligned velocity distribution in the tailward direction, which is the only direction with good statistics at high latitude (enough events; cf Figure 4). Specifically:

$$\text{along } -x \text{ and at } \beta < 0.1: \quad \langle \langle 2\, v_{\parallel}^2(O^+) \rangle \langle v_{\perp}^2(O^+) \rangle^{-1} \rangle = 6 \quad \pm 1$$

$$\text{along } -x \text{ and at } \beta > 0.1: \quad \langle \langle 2\, v_{\parallel}^2(O^+) \rangle \langle v_{\perp}^2(O^+) \rangle^{-1} \rangle = 2.4 \pm 0.1$$

where the inner brackets $\langle\rangle$ indicate mean of velocity distribution and the outer $\langle\rangle$ mean of samplings. (The "2" in the numerator compensates for the single degree of freedom.)

Notes on the He^{++} Ions

At first glance, it may seem strange that a *plasma sheet* ion population of presumed solar origin, like the He^{++}, would be found flowing tailward essentially along Earth's magnetic field, as implied by Figure 3. Even "stranger" is the observation that the tailward direction is the preferred one at $\beta < 0.1$. One might well suspect some instrumental effect, whereby the He^{++} signal is caused by H^+ ions of terrestrial origin. That *no such* instrumental effect is responsible is demonstrated by the time-averaged mass spectra in Figure 5. These mass spectra are from the very same instrument cycles that entered into Figures 2, 3 and 4. The He^{++} mass peak, the second from right in each panel, is very narrow (~three mass channels) and well separated from the strong H^+ peak on the right (a feature of the optimal instrument design).

A second important feature of Figure 5 is that the He^{++} peak is larger than the He^+ peak (second from left). This is contrary to what would be expected with a terrestrial origin, since He^{++} ions are *far less common* in ionospheric ion outflows than are the He^+ ions [e.g. *Collin et al.*, 1988].

As far as the solar origin of both the He^{++} and the H^+ ions is concerned, it is interesting to note that the mean (~thermal) energy of tailward flowing ($-x$) H^+ ions at $\beta < 0.1$ in Table 4 is barely above the typical bulk flow energy of H^+ ions in the solar wind (~1 keV at 440 km s^{-1}), indicating almost pure thermalization of incoming solar wind ions. As seen by the corresponding He^{++}/H^+ energy ratios in Table 6, the same is true of He^{++} ions, as well (the two species have nearly the same flow speed in the solar wind, typically somewhat above 400 km s^{-1}, and the He^{++} ions therefore about four times the energy). In this case the He^{++} mean energy, which is much less susceptible to poor counting statistics than the drift velocity, is based on the *same* plasma samplings used for the H^+ ions.

The mostly solar origin of the He^{++} and H^+ ions is further corroborated by the corresponding concentration ratios in Table 7, where again the *same* plasma samplings are used for both (see e.g. *Feldman et al.* [1978] for typical 3-5% solar wind ratios).

Figure 6 shows the spatial location, in GSM coordinates, of all (left) tailward and (right) earthward field-aligned flows of He^{++} ions from Figure 3. The tailward flows are most common near the plasma sheet dawn and dusk flanks, but they do occur clear across the nightside.

Table 4. Mean Energy (keV; Drift + Thermal) of H^+ With Given Drift Direction

	IMF $B_z \geq 0$ Dawn and Dusk Combined		
	$+x$	$\pm y$	$-x$
$\beta < 0.1$:	3.6 ± 0.1	1.70 ± 0.08	1.32 ± 0.06
$\beta > 0.1$:	3.21 ± 0.05	3.05 ± 0.05	2.78 ± 0.06
	IMF $B_z < 0$ Dawn and Dusk Combined		
	$+x$	$\pm y$	$-x$
$\beta < 0.1$:	4.7 ± 0.1	2.3 ± 0.1	1.42 ± 0.05
$\beta > 0.1$:	4.42 ± 0.07	4.14 ± 0.06	3.39 ± 0.09

Table 5. Parallel (×2) to Perpendicular Mean Energy Ratio of H^+

	IMF $B_z \geq 0$ and < 0 and Dawn and Dusk Combined		
	$+x$	$\pm y$	$-x$
$\beta < 0.1$:	1.97 ± 0.05	1.10 ± 0.02	1.29 ± 0.05
$\beta > 0.1$:	1.31 ± 0.01	1.12 ± 0.01	1.15 ± 0.01

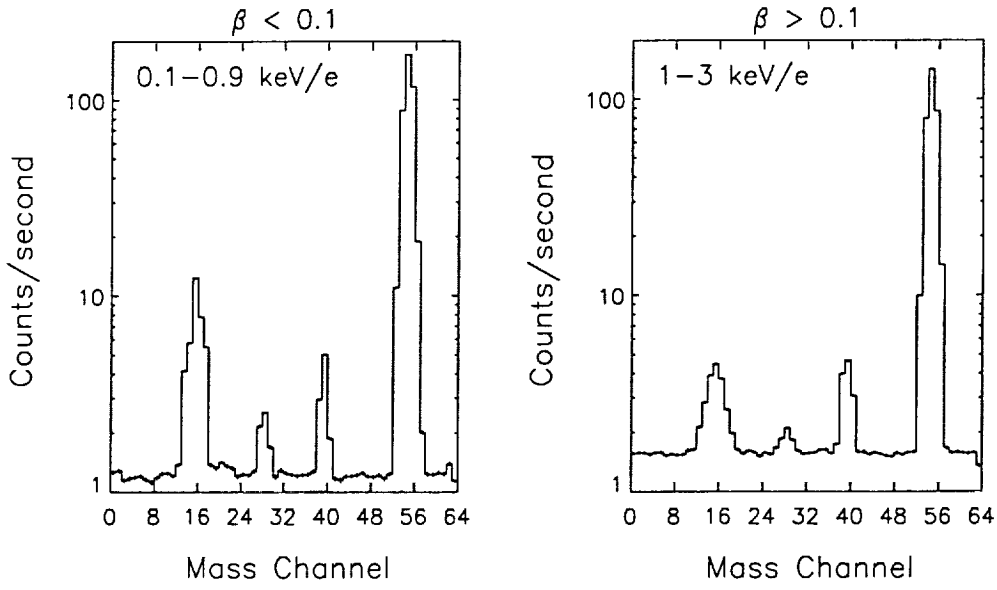

Figure 5. Sample mass spectra (partial energy ranges) averaged over the same time frame as Figure 2 (~4.5 years) at (left) high and (right) intermediate latitude. The four mass peaks in each frame are, from left to right, O^+, He^+, He^{++} and H^+ ions.

Table 6. He^{++}/H^{+} Ratio of Mean Energies With Given H^{+} Drift Direction

	IMF $B_z \geq 0$ Dawn and Dusk Combined		
	$+x$	$\pm y$	$-x$
$\beta < 0.1$:	2.8 ± 0.1	4.0 ± 0.3	4.2 ± 0.2
$\beta > 0.1$:	3.10 ± 0.04	3.30 ± 0.04	3.19 ± 0.05

	IMF $B_z < 0$ Dawn and Dusk Combined		
	$+x$	$\pm y$	$-x$
$\beta < 0.1$:	2.8 ± 0.1	3.7 ± 0.2	4.4 ± 0.4
$\beta > 0.1$:	2.79 ± 0.04	3.06 ± 0.05	3.14 ± 0.08

Table 7. He^{++}/H^{+} Ratio (%) of Number Densities With Given H^{+} Drift Direction

	IMF $B_z \geq 0$ Dawn and Dusk Combined		
	$+x$	$\pm y$	$-x$
$\beta < 0.1$:	3.8 ± 0.8	4.4 ± 0.7	3.5 ± 0.3
$\beta > 0.1$:	2.3 ± 0.1	2.5 ± 0.2	2.4 ± 0.1

	IMF $B_z < 0$ Dawn and Dusk Combined		
	$+x$	$\pm y$	$-x$
$\beta < 0.1$:	2.1 ± 0.6	4.3 ± 0.7	4.8 ± 0.4
$\beta > 0.1$:	1.7 ± 0.1	2.2 ± 0.4	3.1 ± 0.6

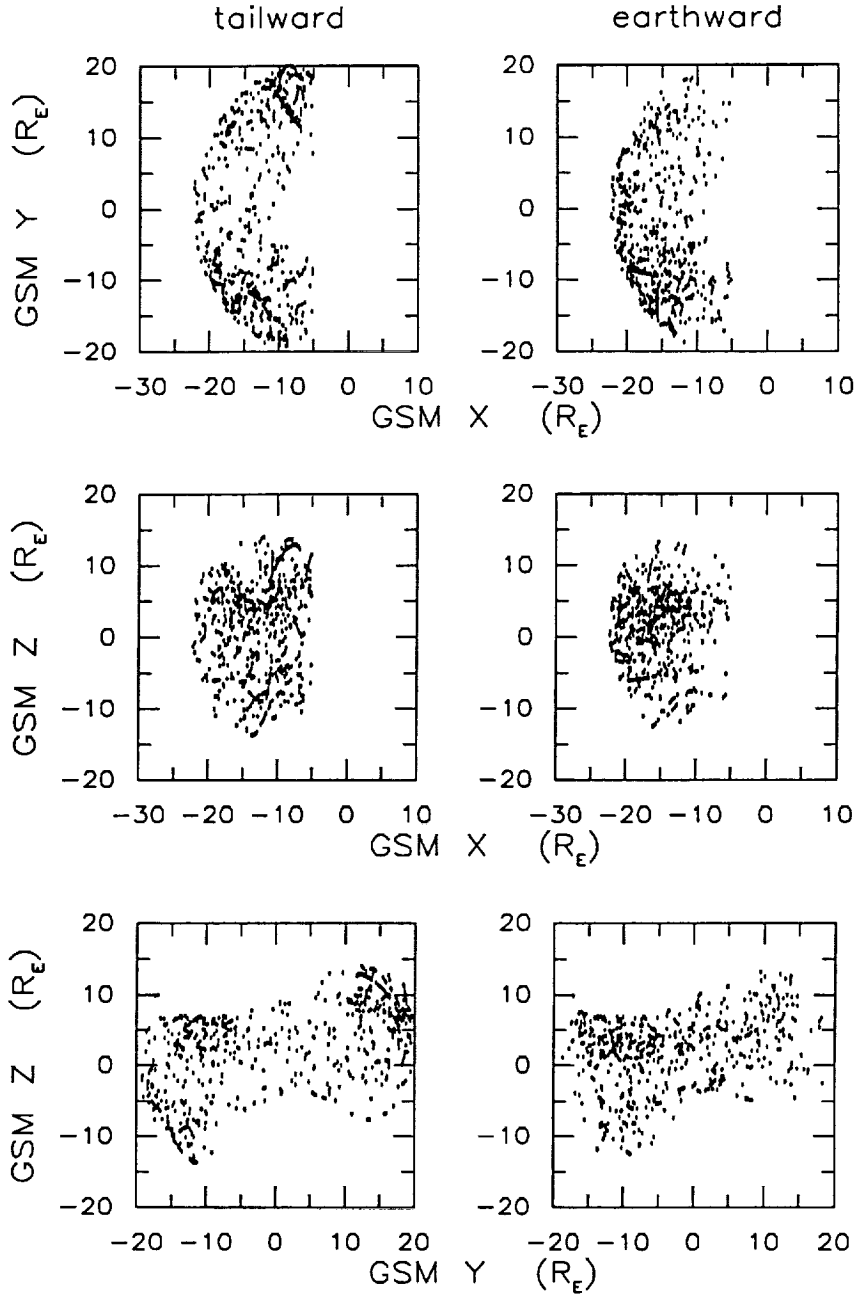

Figure 6. Location in GSM coordinates of the "field-aligned" portion of the He^{++} drift angles in Figure 3, which means (left) 180° ±30° and (right) 0° ± 30°. The slight "tilt" of the point pattern in the bottom panels is a seasonal sampling effect, with points near dawn being from winter, when Earth'north magnetic pole is most often tilted away from Sun, and points near dusk being from early summer. This figure combines high and intermediate latitudes (all beta).

Notes on the Earthward (+x) H^+ Flows

As mentioned above with reference to Table 3, the largest H^+ drift *speeds* are usually observed in the earthward field-aligned direction, especially at high latitude ($\beta < 0.1$). The same tends to be true of He^{++} ions as well, but their statistics are marginal (fewer significant measurements), as is the case with O^+ ions in the earthward flow direction. In the case of the more abundant H^+ ions, the observations do not seem to be of true earthward field-aligned "flows", however, but rather of transient *bursts* and associated *velocity dispersion*, as already noted in the review article in Appendix I (Section 5).

Stated differently, the fastest (most energetic and most field-aligned) H^+ ions of rather *low density* often reach the ISEE-1 satellite while the lower energy H^+ ions are still few or missing (low β), and may supply the sole contribution to many H^+ samplings (~few min each), on which the velocity moments are subsequently based. Such samplings tend to bias the average drift velocity, and they are *only* taken in the earthward direction.

Another angle on this issue is provided by the peak count rates per instrument cycle, which are part of the archived data files. These rates were recorded for each *M/Q* and *E/Q* as measures of possible "beam-like" distributions occuring during a given cycle. These are proportional to peak differential number flux at low energy (due to pre-acceleration) and differential energy flux at high energy. Table 8 shows averages of the H^+ phase space densities corresponding to each maximum count rate per cycle (largest peak among all energy steps), sorted according to its direction of ion motion. Table 9 shows the corresponding average energy at peak count rate. As can be seen, the peaks in the earthward direction at $\beta < 0.1$ are the ones with the highest energy but with the lowest phase space density, an effect that is consistent with a velocity distribution that often lacks a low-energy part because of velocity dispersion.

3.1.2. RESULTS WITH ALL DRIFT VELOCITIES

To obtain a fair measure of ion flow *densities* it is necessary to remove the restriction on drift velocities, which may in fact be near zero part of the time, and to allow less precise directional measurements. Lack of angular precision in a given sampling, when velocity is *not small*, is always due to low ion density (low count rates), and that is then naturally compensated for by a low density weight on that sampling in the final average. Unfortunately, the archival data base used here does not list number flows per se, only number densities and drift velocities. The number densities, which are linear functions (weighted sums) of counts, may have negative values, caused by the subtraction of detector background counts. Such samplings have no meaningful velocities, and the corresponding positions in the data files have dummy fill. This is more likely to be the situation for minor ions, which means that their full data bases are somewhat smaller than that for H^+ ions.

Table 10 lists the net average flows among all samplings at high and intermediate latitudes (and all GSM *y*) with the tailward direction as reference. The consistently tailward flow of O^+ ions is no doubt real, in view of the field-aligned nature of the O^+ velocity distribution, but the flow of He^{++} ions may not be tailward at $\beta > 0.1$ with negative IMF B_z, as shown, considering that the net H^+ flow is earthward there. The difference between He^{++} and H^+ ions in this regard may reflect the problem of having slightly different number of samplings. In any case, the flows at $\beta < 0.1$ are *tailward* and substantial for *all* species.

3.2. Near-Equatorial Latitude (Central Plasma Sheet)

In this region the instrument provides only limited pitch-angle coverage (large pitch angles), and the ecliptic projection of the local magnetic field becomes less relevant. Flow directions have therefore been derived in standard GSE *x-y* components without adjustment for the B_x-B_y angle.

Table 11, also based on significant ($> 2.5\sigma$) velocity measurements, is thus analogous to Table 1,

Table 8. H^+ f(v) (10^5 s^3 km^{-6}) at Peak Count Rate per Instrument Cycle

	IMF $B_z \geq 0$ Dawn and Dusk Combined		
	$+x$	$\pm y$	$-x$
$\beta < 0.1$:	3.0 ± 0.6	23 ± 2	20 ± 4
$\beta > 0.1$:	19 ± 3	22 ± 2	28 ± 4

	IMF $B_z < 0$ Dawn and Dusk Combined		
	$+x$	$\pm y$	$-x$
$\beta < 0.1$:	2.9 ± 0.4	21 ± 2	19 ± 3
$\beta > 0.1$:	9 ± 1	20 ± 3	21 ± 4

Table 9. H^+ Energy (keV) at Peak Count Rate per Instrument Cycle

	IMF $B_z \geq 0$ Dawn and Dusk Combined		
	$+x$	$\pm y$	$-x$
$\beta < 0.1$:	3.8 ± 0.2	0.48 ± 0.04	0.57 ± 0.07
$\beta > 0.1$:	2.74 ± 0.09	2.1 ± 0.1	2.09 ± 0.09

	IMF $B_z < 0$ Dawn and Dusk Combined		
	$+x$	$\pm y$	$-x$
$\beta < 0.1$:	6.2 ± 0.3	0.79 ± 0.07	1.1 ± 0.1
$\beta > 0.1$:	4.6 ± 0.2	3.4 ± 0.2	3.0 ± 0.1

Table 10. Net Tailward ($-x$) Flows ($m^{-2}\ s^{-1}$) of Ions With Arbitrary Drift Speed

	IMF $B_z \geq 0$ Dawn and Dusk Combined		
	H^+	He^{++}	O^+
$\beta < 0.1$:	$(1.4 \pm 0.1) \times 10^9$	$(9 \pm 1) \times 10^7$	$(8.4 \pm 0.2) \times 10^8$
$\beta > 0.1$:	$-(1.6 \pm 0.3) \times 10^9$	$(1 \pm 1) \times 10^7$	$(9.2 \pm 0.2) \times 10^8$
	IMF $B_z < 0$ Dawn and Dusk Combined		
	H^+	He^{++}	O^+
$\beta < 0.1$:	$(2.3 \pm 0.1) \times 10^9$	$(1.6 \pm 0.1) \times 10^8$	$(1.99 \pm 0.03) \times 10^9$
$\beta > 0.1$:	$-(1.1 \pm 0.3) \times 10^9$	$(3 \pm 1) \times 10^7$	$(1.12 \pm 0.03) \times 10^9$

Table 11. Net Dawnward (–GSE y) Drift Velocity (km s^{-1}) With Tail $|B_z| > (B_x^2+B_y^2)^{1/2}$

	IMF $B_z \geq 0$					
	Dawn			Dusk		
	H^+	He^{++}	O^+	H^+	He^{++}	O^+
$\beta > 0.1$:	4 ± 1	2 ± 2	-5 ± 2	-8 ± 1	-11 ± 4	-8 ± 2

	IMF $B_z < 0$					
	Dawn			Dusk		
	H^+	He^{++}	O^+	H^+	He^{++}	O^+
$\beta > 0.1$:	7 ± 1	-5 ± 7	-3 ± 2	-10 ± 2	-21 ± 16	-12 ± 4

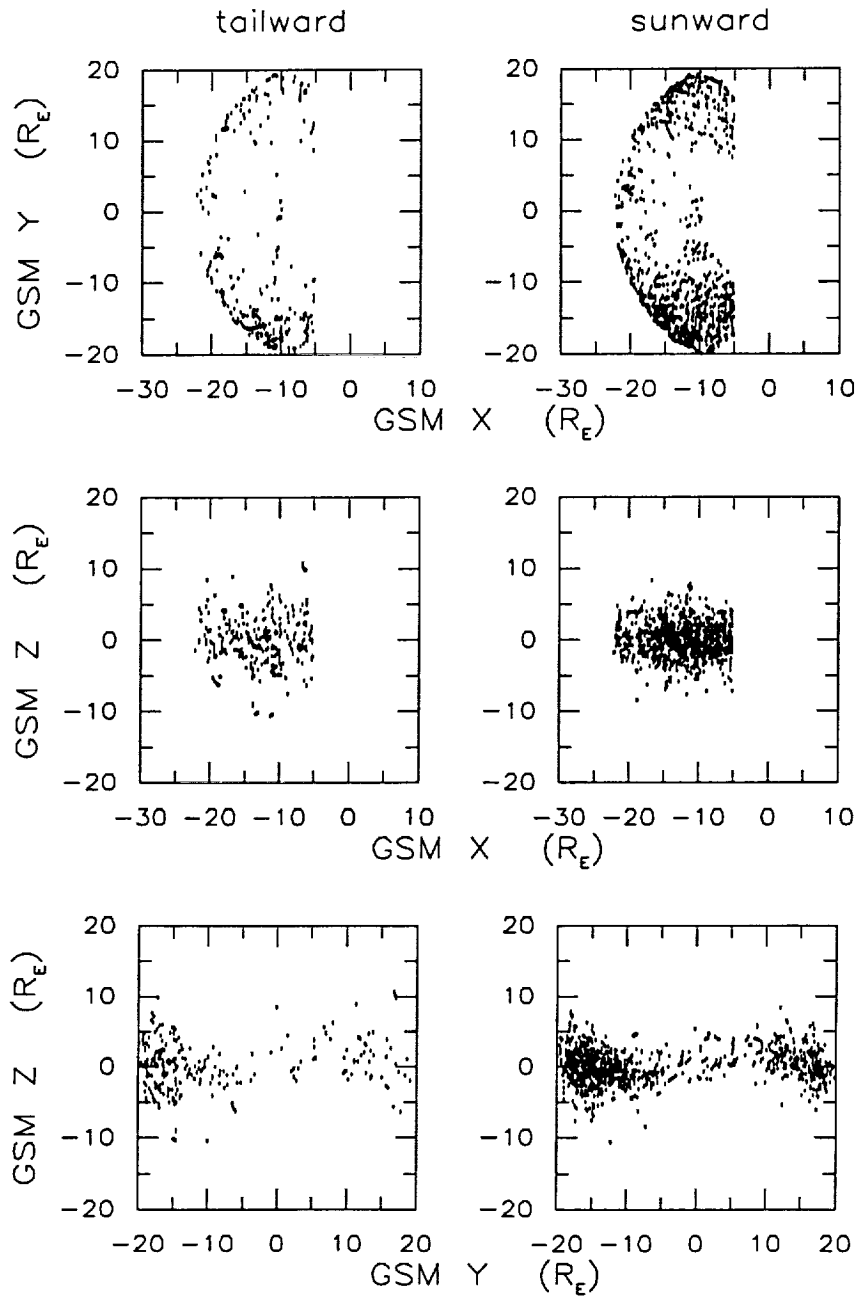

Figure 7. Location in GSM coordinates of Sun-Earth aligned, to within ±30°, H^+ drifts (> 2.5σ; along GSM and GSE *x*-axis) in *central* plasma sheet, as defined by $|B_z| > (B_x^2+B_y^2)^{1/2}$.

Table 12. Net Sunward (+GSE x) Flows ($m^{-2}\ s^{-1}$) With Tail $|B_z| > (B_x^2+B_y^2)^{1/2}$

	IMF $B_z \geq 0$ Dawn and Dusk Combined		
	H^+	He^{++}	O^+
$\beta > 0.1$:	$(3.1 \pm 0.6) \times 10^9$	$(6 \pm 3) \times 10^7$	$(6 \pm 3) \times 10^7$
	IMF $B_z < 0$ Dawn and Dusk Combined		
	H^+	He^{++}	O^+
$\beta > 0.1$:	$(8.4 \pm 0.4) \times 10^9$	$(2.1 \pm 0.2) \times 10^8$	$(5.7 \pm 0.3) \times 10^8$

except that the drift direction refers to the dusk-to-dawn axis, not local East. As in Table 1 at $\beta > 0.1$, there is a preference for drift away from the tail center, although with larger statistical variations. This trend may be due mostly to samplings off the equatorial plane proper, being that such drift within that plane corresponds to poleward **E**×**B** drift in the ionosphere, as implied by Figure 1. In other words, sunward drift at constant magnetic latitude in the ionosphere corresponds to sunward drift in the equatorial plane itself, as well (if magnetic field lines are essentially equipotentials).

In like manner, Figure 7 is analogous to Figure 6, except that the $\pm x$-drift refers to the GSE (and GSM) x-axis, not the local magnetic field-aligned axis, and it shows H^+ drift. Like Figure 6, it includes samplings without regard to concurrent solar wind conditions.

A striking difference from Figure 6 is the relative frequency of occurrence of tailward versus sunward (earthward) drifts. If these occurrences are counted by $N(v_x<0)$ and $N(v_x>0)$, respectively, the ratio is $N(v_x>0)/N(v_x<0) = 3.9$. However, if the samplings are separated by the two-hour IMF B_z polarity, then:

$$\text{IMF } B_z \geq 0: \quad N(v_x>0)/N(v_x<0) = 2.5$$

$$\text{IMF } B_z < 0: \quad N(v_x>0)/N(v_x<0) = 7.5$$

That is, the preference for sunward drift at significant speeds (~enhanced speeds) in the near-equatorial plasma sheet increases threefold during times of southward IMF (as defined by 2.4.1a and 2.4.1b). This is the strongest single effect of a southward turning of the IMF found in this study. This effect is essentially still present when all drift speeds are included, which is shown by the net sunward H^+ flow *densities* in Table 12, along with those of He^{++} and O^+ ions.

4. Discussion

The principal demarcation of ion flow directions in these data is by beta, but $\beta = 0.1$ is not a sharp boundary. This can be seen from Figure 3, for example. The occurrence peak near 180° is much weaker in the bottom than in the top panels, but it is still at <180° in the left bottom panel and at >180° in the right bottom panel, as would be expected with "low-beta" conditions extending into the $\beta > 0.1$ domain. In any case, the "low-beta" He^{++} data, with their preference for tailward field-aligned flows, do raise an issue about the physical interconnection between these samplings and the plasma sheet proper.

Superficially, it might seem that the tailward-flowing He^{++} ions are most likely samplings of the plasma mantle, which bounds the tail lobes on the magnetopause side [e.g. *Rosenbauer et al.*, 1975], rather than samplings of the high-latitude plasma sheet. Being that Figure 3 is based on "significant" velocity measurements, it could in principle be biased by samplings of relatively fast flows among the mantle population. However, the preference for tailward field-aligned drift at $\beta < 0.1$ is shared by the H^+ ions in Figure 2, and the average speed of this drift ($-x$ direction) is not much larger than the average H^+ drift speed perpendicular to the magnetic field (adjusted $\pm y$ directions), as shown by Table 3. In order for the tailward drifting H^+ ions to be mostly in the plasma mantle, Figure 2 then implies that there is a *higher likelihood* to sample the $\beta < 0.1$ conditions in the plasma mantle than in the high-latitude plasma sheet, even though the ISEE-1 satellite roams on a regular basis between the central plasma sheet, where $\beta > 0.1$, and either tail lobe, where $\beta << 0.1$. This does not seem physically possible; encounters with the plasma mantle must be *less frequent* than the passages through the high-latitude edges of the plasma sheet. It may be mentioned that the statistical preference for tailward field-aligned drift of He^{++} and H^+ ions at $\beta < 0.1$ does remain if *no condition* is placed on the velocity measurement (except that it can only be performed if the background-corrected number density is positive), despite a large increase in random drift angles (not shown).

Furthermore, Tables 4 and 5 imply that the field-aligned thermal velocity of H^+ ions is substantially greater than the net tailward drift velocity, so there must be almost as many H^+ ions moving earthward as tailward at any given time, as though on closed magnetic field lines. In any case, this is not consistent with the image of a plasma freely expanding tailward along open mantle field lines.

Additional reasons for discarding the ordinary plasma mantle as the *principal* site of the tailward H^+ flows at $\beta < 0.1$ can be found in the general similarity in Tables 4 through 9 between average parameters of H^+ ions drifting in the $-x$ and $\pm y$ directions; these ions all appear to be the same population drifting at varying angle but preferentially tailward.

It is worth noting, once again, that the tailward flows of H^+ ions at high latitude, like those of He^{++} ions, as well as those of O^+ ions for that matter, must be from a fresh source sunward (and earthward) of the ISEE-1 satellite, rather than being the return flow of ions that have previously been ejected earthward from a distant tail reconnection site and have mirrored closer to Earth. As already pointed out above, the earthward ($+x$) "flows" of H^+ ions that are observed at $\beta < 0.1$ are actually transient bursts, and their peak phase space density is much too low to supply the phase space density of the tailward flows (Table 8; see also Appendix I). This is reflected in the fact that the *net flow density* at $\beta < 0.1$, including all velocity measurements, is indeed *tailward* for all the ions (Table 10).

5. Conclusions

This statistical investigation, using far more samplings of the magnetotail plasma *ion composition* than any previously undertaken, lends further support to the notion that tailward flowing solar origin plasma begins to enter the plasma sheet rather close to Earth [*Lennartsson*, 1992], perhaps as early as the dayside cusp regions, and that it does so whether the IMF B_z is southward or northward. This situation differs substantially from the popular image of just a decade ago, in which the solar origin plasma, at times of southward IMF, descends from the high-latitude magnetosheath into a tail magnetic reconnection site ("neutral line") some 100 R_E downtail, only subsequently to become part of the near-Earth plasma sheet [e.g. *Cowley*, 1980]. This conclusion can be reached from at least three considerations.

(1) As the ISEE-1 satellite roams between the central plasma sheet, where the measured ion beta value often exceeds $\beta \sim 1$, and the tail lobes, where $\beta << 1$, it encounters a transition region of intermediate beta, beginning about $\beta \sim 0.1$, or somewhat larger, and extending to smaller values, where the *predominant* ion flow is tailward, even that of He^{++} ions (Table 10). The tailward drift of He^{++} ions is most pronounced in the dawn and dusk flanks but occurs near local midnight, as well (Figure 6). Ions in this transition region are also found streaming earthward part of the time, at elevated speed and along the magnetic field, most notably the H^+ ions (Table 3; see also Appendix I), as though ejected from a distant reconnection site, but their contribution to the statistically *averaged* flow is minor (cf. Tables 8 and 9).

(2) H^+ and He^{++} ions indeed exhibit their most "solar wind-like" behavior in this transition region, in association with tailward flow, as though of the most recent solar origin (Tables 6 and 7). Conditions here are *not* typical of the plasma mantle, however (Tables 4 and 5).

(3) Cross-field ($\mathbf{E}\times\mathbf{B}$) drift in the transition region tends to be inward, away from the tail flanks, in accordance with the high-latitude arrows in Figure 1 (Figures 2, 3 and 4 and Table 1).

It is important to note that the first and second points depend critically on the knowledge of *ion composition.* Without that knowledge, the tailward (and ~field-aligned) ion flows could be reasonably assumed to be entirely of terrestrial origin.

A new result with important implications for the large-scale plasma sheet dynamics is that the *earthward* flows in the *near-equatorial* plasma sheet increase relatively more with a southward turning of the IMF than do the flows at higher latitude (Table 12 and Section 3.2). This helps explain why

the plasma sheet always thins, and the polar caps increase in size, when the IMF B_z becomes substantially negative (several nT) for some 30 min or longer [*Hones et al.*, 1971]. This thinning effect is well known but poorly understood. It is rather paradoxical within the "standard framework" of reconnection, since a southward turning of the IMF ought to increase the reconnection rate at the magnetopause and, hence, increase the flow of new solar wind plasma *to* the plasma sheet. On the other hand, if the earthward flows near the equator increase more than the inflows of new plasma at higher latitude, as implied by these data, then the plasma sheet *must thin* (cf. speculations on this subject in Section 6 of Appendix I).

6. New Technology

The analysis of data from the Lockheed Plasma Composition Experiment on the NASA/ESA ISEE-1 satellite has been carried out with conventional tools and methods and has not led to the development of new technology, nor was it expected to do so. The data from this instrument, although now made universally accessible in their archived format thanks to the WorldWideWeb, have the same basic scientific application as do data from many other spaceborne plasma analyzers. The only fundamental difference between these and most other space plasma data lies in the separation of ions by mass per charge. Our knowledge about the ion mass composition has so far been utilized for scientific purposes only, and no technological application has yet been envisioned.

References

Collin, H.L., W.K. Peterson, J.F. Drake, and A.W. Yau, The helium components of energetic terrestrial ion upflows: their occurrence, morphology, and intensity, *J. Geophys. Res. 93*, 7558, 1988.

Couzens, D.A., and J.H. King, *Interplanetary medium data book, supplement 3, 1977-1985*, Rep. NSSDC/WDC-A-R&S 86-04, NASA Goddard Space Flight Cent., Greenbelt, Md., 1986.

Cowley, S.W.H., Plasma populations in a simple open model magnetosphere, *Space Sci. Rev., 26*, 217, 1980.

Eastman, T.E., E.W. Hones, Jr., S.J. Bame, and J.R. Asbridge, The magnetospheric boundary layer: Site of plasma, momentum and energy transfer from the magnetosheath into the magnetosphere, *Geophys. Res. Lett. 3*, 685, 1976.

Fairfield, D.H., R.P. Lepping, E.W. Hones, Jr., S.J. Bame, and J.R. Asbridge, Simultaneous measurements of magnetotail dynamics by IMP spacecraft, *J. Geophys. Res., 86*, 1396, 1981.

Feldman, W.C., J.R. Asbridge, S.J. Bame, and J.T. Gosling, Long-term variations of slected solar wind properties: IMP 6, 7, and 8 results, *J. Geophys. Res. 83*, 2177, 1978.

Fujimoto, M., T. Terasawa, and T. Mukai, The cold-dense plasma sheet: A GEOTAIL perspective, *Space Sci. Rev., 80,* 325, 1997.

Hones, E.W., Jr., J.R. Asbridge, and S.J. Bame, Time variations of the magnetotail plasma sheet at 18 R_E determined from concurrent observations by a pair of Vela satellites, *J. Geophys. Res., 76*, 4402, 1971.

Lennartsson, W., A scenario for solar wind penetration of Earth's magnetic tail based on ion composition data from the ISEE 1 spacecraft, *J. Geophys. Res., 97*, 19221, 1992.

Mitchell, D.G., F. Kutchko, D.J. Williams, T.E. Eastman, L.A. Frank, and C.T. Russell, An extended study of the low-latitude boundary layer on the dawn and dusk flanks of the magnetosphere, *J. Geophys. Res., 92*, 7394, 1987.

Orsini, S., M. Candidi, M. Stokholm, and H. Balsiger, Injection of ionospheric ions into the plasma sheet, *J. Geophys. Res., 95,* 7915, 1990.

Rosenbauer, H., H. Grünwaldt, M.D. Montgomery, G. Paschmann, and N. Sckopke, Heos 2 plasma observations in the distant polar magnetosphere: The plasma mantle, *J. Geophys. Res. 80*, 2723, 1975.

Russell, C.T., The ISEE 1 and 2 fluxgate magnetometers, *IEEE Trans. Geosci. Electron., GE-16*, 239, 1978.

Shelley, E.G., R.D. Sharp, R.G. Johnson, J. Geiss, P. Eberhardt, H. Balsiger, G. Haerendel, and H. Rosenbauer, Plasma composition experiment on ISEE-A, *IEEE Trans. Geosci. Electron., GE-16*, 266, 1978.

Tsyganenko, N.A., Global quantitative models of the geomagnetic field in the cislunar magnetosphere for different disturbance levels, *Planet. Space Sci., 35,* 1347, 1987.

Appendix I

Invited ISEE-1 review article
by O.W. Lennartsson

Lockheed Martin Space Systems /Advanced Technology Center
Palo Alto, California

in

Transport Across the Boundaries of the Magnetosphere

Proceedings of an ISSI Workshop
October 1-5, 1996, Bern, Switzerland

Edited by
B. Hultqvist and M. Øieroset
International Space Science Institute, Bern, Switzerland

Kluwer Academic Publishers
Dordrecht /Boston /London

(also in *Space Science Reviews, Vol. 80,* Nos. 1-2, 1997)

ISEE ION COMPOSITION DATA WITH IMPLICATIONS FOR SOLAR WIND ENTRY INTO EARTH'S MAGNETOTAIL

O.W. LENNARTSSON
Lockheed Martin Missiles & Space, Palo Alto, California, USA

Received January 20, 1997; accepted in final form February 6, 1997

Abstract. Energetic (0.1-16 keV/e) ion data from a plasma composition experiment on the ISEE-1 spacecraft show that Earth's plasma sheet (inside of 23 R_E) always has a large population of H^+ and He^{++} ions, the two principal ionic components of the solar wind. This population is the largest, in terms of both number density and spatial thickness, during extended periods of northward interplanetary magnetic field (IMF) and is then also the most "solar wind-like" in the sense that the He^{++}/H^+ density ratio is at its peak (about 3% on average in 1978 and 79) and the H^+ and He^{++} have mean (thermal) energies that are in the ratio of about 1:4 and barely exceed the typical bulk flow energy in the solar wind. During geomagnetically active times, associated with southward turnings of the IMF, the H^+ and He^{++} are heated in the central plasma sheet, and reduced in density. Even when the IMF is southward, these ions can be found with lower solar wind-like energies closer to the tail lobes, at least during plasma sheet thinning in the early phase of substorms, when they are often seen to flow tailward, approximately along the magnetic field, at a slow to moderate speed (of order 100 km s^{-1} or less). These tailward flows, combined with the large density and generally solar wind-like energies of plasma sheet H^+ and He^{++} ions during times of northward IMF, are interpreted to mean that the solar wind enters along the tail flanks, in a region between the lobes and the central plasma sheet, propelled inward by ExB drift associated with the electric fringe field of the low latitude magnetopause boundary layer (LLBL). In order to complete this scenario, it is argued that the rapid (of order 1000 km s^{-1}) earthward ion flows (mostly H^+ ions), also along the magnetic field, that are more typically the precursors of plasma sheet "recovery" during substorm expansion, are not proof of solar wind entry in the distant tail, but may instead be a time-of-flight effect associated with plasma sheet redistribution in a dipolarizing magnetic field.

Key words: Magnetotail, Plasma Sheet, Low Latitude Boundary Layer, Solar Wind Entry, Tail Plasma Flows, Substorms

Abbreviations: ISEE-International Sun-Earth Explorer, GSM-Geocentric Solar Magnetospheric, GSE-Geocentric Solar Ecliptic, R_E-Earth Radii, IMF-Interplanetary Magnetic Field, LLBL-Low Latitude Boundary Layer, AE-Auroral Electrojet Index, NSSDC-National Space Science Data Center, NASA-National Aeronautics and Space Administration

1. Introduction

The plasma composition experiment on the International Sun-Earth Explorer One (ISEE-1) spacecraft (Shelley *et al.*, 1978) provided the first tool for *in situ* determination of the chemical makeup of Earth's plasma sheet, from its inner edge out to a geocentric distance of almost 23 R_E. By the time of the ISEE-1 (and ISEE-2) launch, on October 22, 1977, there had been mounting recent evidence that the

Space Science Reviews **80**: 305–323, 1997.

energetic (hundreds of eV to tens of keV) plasmas in Earth's magnetosphere have not only a solar wind source, as previously thought, but also a very significant terrestrial source, as manifested by singly charged oxygen at keV energies (*e.g.* Shelley *et al.*, 1972; Ghielmetti *et al.*, 1978; Balsiger *et al.*, 1980, and references therein). Those findings had made it eminently clear that the whereabouts of solar origin plasmas in the magnetosphere are a matter of chemistry, and that future space plasma probes would have to include instruments capable of separating different ions. The ISEE-1 instrument were to provide a wealth of new information over the next 4 1/2 years, some of it rather surprising, not only about the plasma sheet, but about plasmas in various regions between the inner magnetosphere and the magnetopause boundary layers and beyond (*e.g.* Sharp *et al.*, 1983). This article focuses on the tail region and, in particular, on data that seem to have the strongest bearing on the entry of solar wind particles into the plasma sheet.

The principal background material for this article can be found in a single study by Lennartsson (1992), henceforth referred to as Paper I. Those issues that were discussed at length in Paper I are treated only briefly here, with minimal use of the same figures, in order to leave more room to elaborate on certain important issues that have since been clarified through further analysis of the same data.

Recent statistical analysis of the ISEE-1 ion composition data has made extensive use of a particular set of compacted archival data being prepared for the public domain. The format of these is described in Lennartsson (1994; Appendix A2). That same publication also has a fairly detailed description of the instrument and its operation and performance in flight (Appendix A1). Further information can be obtained on the Internet WWW page ftp://sierra.space.lockheed.com/DATA /isee/Welcome.html.

1.1. RELEVANT INSTRUMENT PROPERTIES

The ISEE-1 instrument is similar to early spaceborne electrostatic particle analyzers with a rather limited instantaneous field of view, pointing approximately perpendicularly to the spacecraft spin axis, except that it has both a conventional analyzer of total ion flux, at a given energy per charge, and a subsequent section which only records ions of a given mass per charge. Obtaining energy spectra of various major and minor ions thus amounts to electronically stepping through both energy and mass, including detector noise measurements (while blocking all ions). Allowing for the 3-sec spin period of ISEE-1 to provide the angular ion flux information, the practical cycle time is usually some 8 to 17 minutes. By utilizing the "total ion" count rate and assuming that H^+ ions are strongly dominant, which they often are, it is possible to obtain H^+ bulk properties at 1-3 minutes time resolution in all modes of operation.

The field of view (the size of which varies with ion energy; see Shelley *et al.*,

1978) is centered in the spin plane for the "total ion" analyzer, which means approximately along the solar ecliptic plane, and 5° below the spin plane for the mass analyzer. Consequently, it is possible to obtain full pitch-angle coverage only in regions where the magnetic field is nearly parallel to the solar ecliptic plane, which often does include the tail lobe boundaries of the plasma sheet, but usually not the central plasma sheet. Furthermore, in order to derive number densities and higher order velocity moments, it is necessary to make assumptions about the ion velocity distributions at angles well away from the ecliptic plane. Various assumptions have been applied to different regions, as discussed in Paper I (see also Appendix A2 in Lennartsson, 1994).

The energy range of data presented here, unless stated differently in some case, is about 100 eV/e to 16 keV/e. This is only a marginally sufficient range in the hottest parts of the plasma sheet, and it does have a somewhat biasing effect on the comparison of H^+ and He^{++} ions, since they tend to have nearly equal mean energy per nucleon, as opposed to equal energy per charge (see Lennartsson and Shelley, 1986). The effect is essentially negligible when their number densities are compared (*i.e.* with only 0:th order velocity moments involved), except when the He^{++} measured mean energy is well above 3 keV/nucleon, in which case the He^{++}/H^+ ratio does become artificially low, but there is a noticeable underestimation of the true He^{++} mean energy even at measured values of 3-4 keV/nucleon (typical case).

1.2. SUPPLEMENTARY DATA

The analysis of the ion composition data requires extensive use of magnetic field data from the ISEE-1 fluxgate magnetometer (Russell, 1978), both for pitch-angle calculations and for the physical classification of the plasma as a whole, including its beta value.

For the intercomparison with solar wind conditions, a large set of hourly averaged solar wind velocity moments (protons and electrons) and interplanetary magnetic field (IMF) components have been extracted from the NSSDC/OMNI tape records (Couzens and King, 1986). About 70% of the ISEE-1 plasma sheet data has concurrent solar wind and IMF data in the OMNI file.

The principal measure of geomagnetic activity has been the hourly AE index, also extracted from a magnetic tape (*cf.* Kamei and Maeda, 1982, and adjoining data books).

2. Evidence of Solar Wind Entry Into Earth's Magnetotail

Figure 1 illustrates some of the main arguments made in Paper I in favor of a strong presence of solar origin plasma in the plasma sheet, especially during ex-

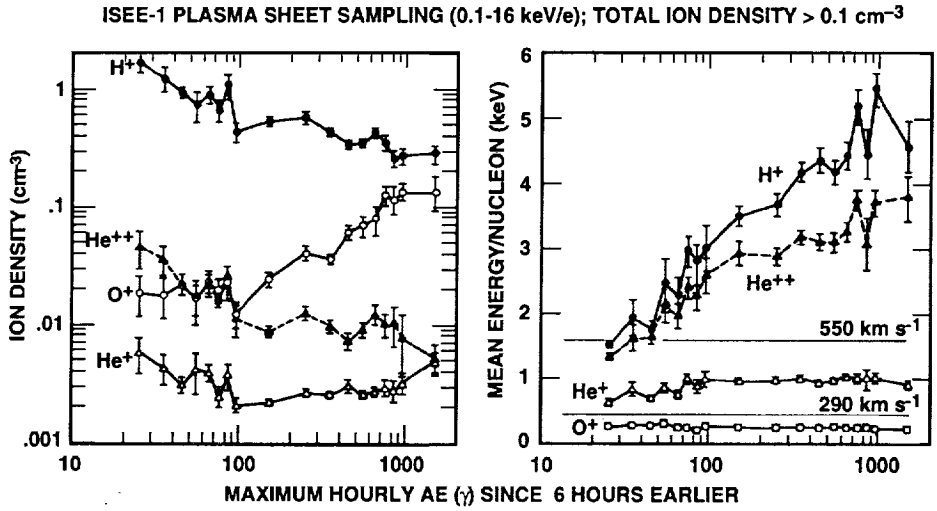

Figure 1. Central plasma sheet densities (left) and mean energies (right) of the four major ions, averaged over space and sorted according to the maximum level of auroral electrojet (AE) activity during the sampling and the preceding 6 hours. The thin horizontal lines in the right panel indicate the range of energy per nucleon that corresponds to the most common range of solar wind speeds. Error bars in this figure, and in Figures 2 and 7 below, show ± 1 σ of the mean (from Paper I).

tended periods of extreme geomagnetic quiescence:

(1) The He^{++} is almost always substantially more abundant than the He^{+}, in spite of the fact that the latter is a more common component of the known outflow of ions from Earth's polar regions (*e.g.* Collin *et al.*, 1988).

(2) The He^{++} concentration is generally well correlated with that of the H^{+}, but poorly correlated, and in part even anti-correlated, with the He^{+} and O^{+} concentrations.

(3) The He^{++}/H^{+} number density ratio, about 2% - 3% on average, is almost as high as the corresponding ratio in the solar wind (3% - 5% during the relevant solar cycle phase; *c.f.* Feldman *et al.*, 1978).

(4) The He^{++} and H^{+} mean energies, in terms of keV/nucleon, are similar to each other, but very different from either of the He^{+} and O^{+} energies. The similarity between the He^{++} and H^{+} energies becomes very close if those energies are corrected for the finite energy window of the data (Lennartsson and Shelley, 1986).

The third point should be viewed in the context of two complementary effects, namely the admixture of terrestrial H^{+} and the preferential entry of H^{+} over He^{++} from the solar wind. According to recent findings by Fuselier *et al.* (1997), the latter effect may be the dominant one, at least when the solar wind contribution to the absolute plasma density is particularly strong. As Figure 1 suggests, based on the He^{++} density, for instance, that tends to occur during times of very low AE.

A somewhat paradoxical aspect of Figure 1 is the anti-correlation between the density of solar origin ions and the AE index, since a weak AE tends to occur with a northward IMF, which has long been associated with a "closed" magnetopause. In fact, if the data are sorted according to the polarity of the concurrent hourly IMF B_Z (in GSM coordinates), as done in Figure 5 of Paper I, the plasma sheet He^{++} and H^+ densities are seen to increase with increasing solar wind (proton) density in a roughly proportional fashion for positive (northward) B_Z but to increase at a slower rate (or not increase at all) for negative B_Z. A similar result has been obtained recently with the Geotail spacecraft by Fujimoto *et al.* (this issue), using an electrostatic ion analyzer (and assuming H^+ ions).

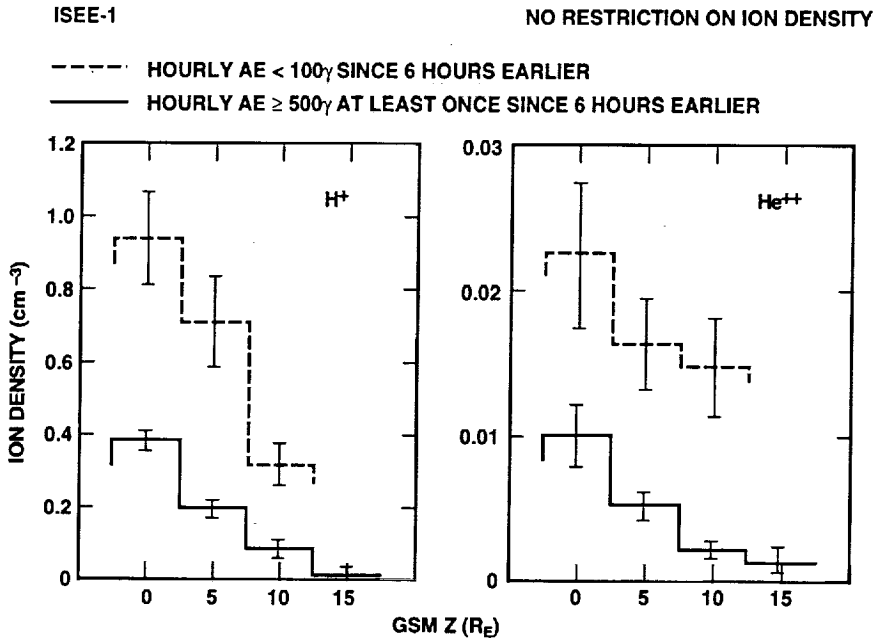

Figure 2. Densities of (left) the H^+ and (right) the He^{++} during quiet (dashed lines) and active conditions (solid lines), sorted according to the geocentric solar magnetospheric (GSM) z coordinate. The averages include samplings from the northern lobe here (from Paper I).

This result, however, should have been anticipated, since early studies of the plasma sheet dynamics by Hones *et al.* (1971), using energetic electron data, indicated that the plasma sheet at 18 R_E becomes hotter and less dense after a substorm, that is after the plasma sheet has "recovered", following the initial transient thinning, which typically lasts less than 2 hours. Being that the H^+ is usually the dominant positive component, the behavior of its density and mean

energy in Figure 1 merely supports the findings by Hones *et al.*(1971) and shows that the substorm-induced changes become increasingly pronounced with increasing substorm activity.

Figure 2 shows more specifically the effects of substorms on the plasma sheet content of solar origin ions by extending the measurements into the northern tail lobe (allowing samplings with combined ion density < 0.1 cm^{-3}). Clearly, the reduction in the H^+ and He^{++} densities during disturbed times, even after plasma sheet "recovery" (AE spanning well over 2 hours), affects the bulk of the plasma sheet (at least inside the ISEE-1 apogee at 23 R_E). The conclusion drawn from this is that the plasma sheet must become refilled by solar wind-like (cooler) plasma between periods of geomagnetic activity, thus including extended periods of northward IMF. The entry process may well be operating during active times, as well, but some loss process is then temporarily activated or enhanced.

It should perhaps be emphasized at this point that, although the upper energy cutoff at 16 keV/e does conspire with the increasing bulk energies to reduce the measured number density of both the H^+ and the He^{++} during strong substorm activity, the effect demonstrated by Figures 1 and 2 is far greater than can be attributed to instrumental effects (see Lennartsson and Shelley, 1986, for a discussion of that topic).

3. Tailward Flows of Solar Origin Ions Adjacent to the Plasma Sheet

Paper I dealt rather extensively with events of slow (mostly < 200 km s^{-1}) but dense (H^+ number density on average 1 cm^{-3}) tailward flows of ions observed immediately preceding the onset of moderately strong substorms (*cf.* Huang *et al.*, 1992), and the primary objective was to determine their origin. Figure 3 shows the location of the 23 events studied.

With the possible exception of two or three, these events appear to be located between the plasma sheet proper and the adjacent tail lobe and to have been brought into view by the initial thinning of the plasma sheet prior to the substorm expansive phase (*cf.* Hones *et al.*, 1971). Based on the densities and mean energies of the various ionic components, the H^+ being at least ten times denser than the others, it was concluded that the dominant plasma source must have been the solar wind, rather than Earth's ionosphere. Specifically, the 23 pairs of total energies E of He^{++} and H^+ ions, adding thermal and bulk flow energies as measured (without correction for the finite energy window), are statistically related by

$$E(He^{++})/E(H^+) = 3.7 \pm 0.7$$

with a correlation coefficient of 0.9 (the "±" refers to the standard deviation of points here), while the corresponding comparison of O^+ and H^+ ions yields

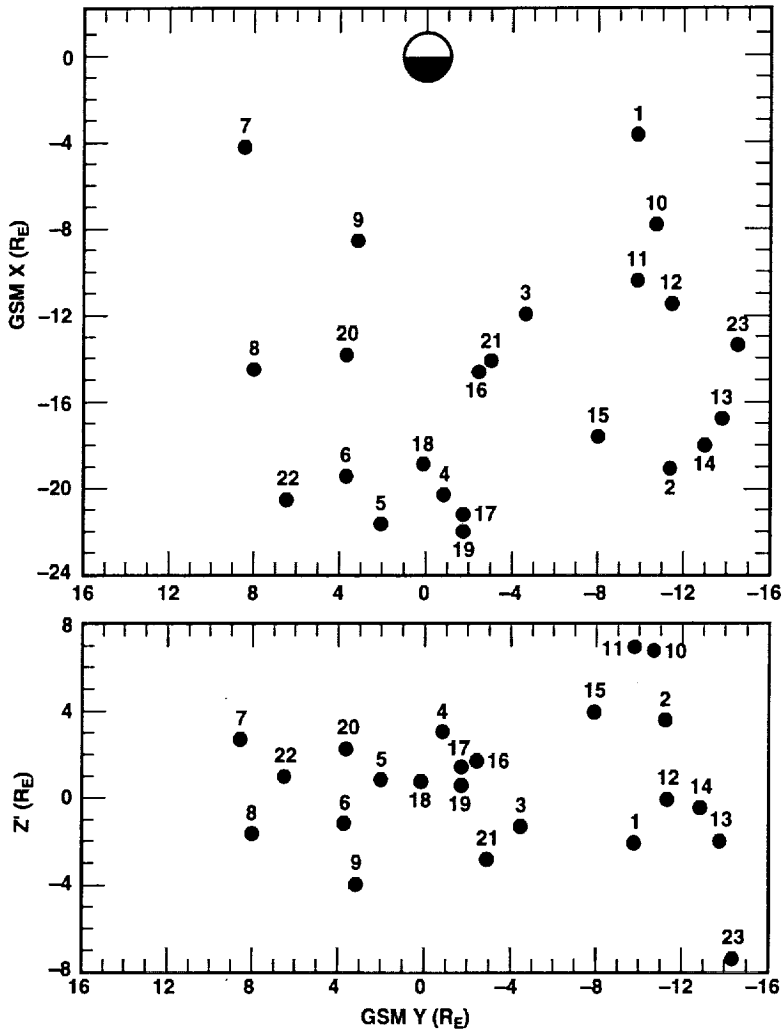

Figure 3. Location of events of tailward flowing H^+ and He^{++} ions. Top panel shows location in GSM x versus y; bottom panel shows distance above and below nominal "neutral sheet", as defined by Fairfield and Ness (1970; from Paper I).

$$E(O^+)/E(H^+) = 2.1 \pm 2.1$$

with a correlation coefficient of only 0.1. The energy of the H^+ ions is about 1 keV or less in almost half of the events, indicating that the bulk flow of the solar wind can be converted to thermal energy with little or no net heating during entry.

Since there is no sign of substantial earthward flows in conjunction with these events, it was concluded that they are probable evidence of solar wind entry sun-

ward of the ISEE-1 position at those times.

4. Inferred Large-Scale Plasma Flows

Figure 4 is analogous to Figure 13b in Paper I, except that it relates, in a schematic fashion, the inferred cross-tail E×B drift to high-latitude convection cells in the ionosphere.

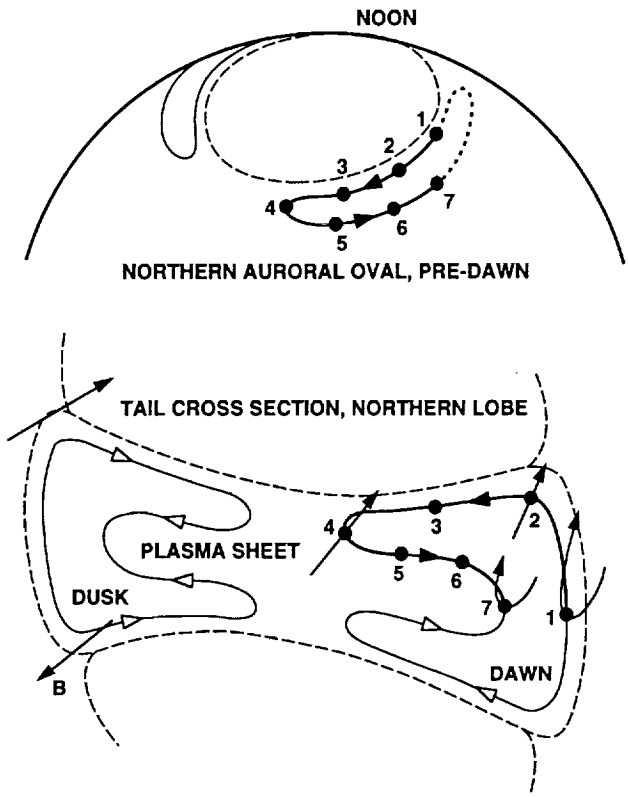

Figure 4. Upper portion shows hypothetic convection cells in the ionosphere (flow direction indicated by arrow heads), located entirely on magnetic field lines that interconnect the two hemispheres. The dashed oval-shaped contour indicates the equatorward boundary of field lines leading into the northern tail lobe. Lower portion shows, qualitatively, the corresponding convection contours in a tail cross section (**B** denotes a magnetic field vector), assuming a purely geometric mapping along the magnetic field. The numbered points correspond, one by one, with the numbers along the ionospheric convection cell. Points 1 and 7 lie on the two most sunward field lines long enough to reach this particular tail cross section. Points 1 and 2 are assumed to lie within the low latitude magnetopause boundary layer (LLBL). The remaining three "horns" in the tail convection have analogous connections to the ionosphere. The dashed lines represent the magnetopause and the interface between the plasma sheet and the lobes (adapted from Paper I).

The cross-tail equipotential contours in this figure provide a means to close those associated with the dusk-dawn directed electric field in the low latitude magnetopause boundary layer (LLBL) on the tail flanks (*cf.* Eastman *et al.*, 1976; Mitchell *et al.*, 1987). The particular shape accounts for two aspects of observed cross-tail plasma flows: 1. the deviation from pure magnetic field-alignement of tailward streams of very cold O^+ ions indicates the presence of **E×B** drift directed away from the nearest flank toward the tail center in a region between the lobes and the plasma sheet proper (*e.g.* Orsini *et al.*, 1990), while 2. the corresponding alignment of O^+ streams further inside the plasma sheet (Orsini *et al.*, 1990), as well as bulk flows of the hot H^+ population there (Figure 14 in Paper I), indicate **E×B** drift in the reverse direction. This is equivalent to having a sheet of net electric charge of the same polarity as the inside of the adjacent LLBL, that is positive at dawn, negative at dusk (*cf.* Eastman *et al.*, 1976), extend into the tail between the lobes and the central plasma sheet. Such a charge distribution would result, at least in the near-Earth plasma sheet, from the LLBL charges propagating earthward along the magnetic field, although the **E×B** drift may also carry with it a net charge.

Besides being in crude agreement with actual observations, direct and indirect, of cross-tail particle drift, this kind of flow pattern might explain why tailward flows of solar wind-like ions can be found along the ISEE-1 orbit, well inside of the nominal magnetopause, as outlined in the preceding section. This assumes that the LLBL contains newly trapped solar wind plasma, as suggested by observations (Eastman *et al.*, 1976; Mitchell *et al.*, 1987), and that it is at least partially located on closed geomagnetic field lines (*e.g.* Mitchell *et al.*, 1987). The latter would enable part of the LLBL plasma, along its junction with the lobe magnetopause boundary layer (*i.e.* the "plasma mantle"; Rosenbauer *et al.*, 1975) to enter into the tail (at Point 2, for instance). With a typical inward convection speed of a few tens of km s^{-1} (Orsini *et al.*, 1990), this plasma may reach the center of the tail in the course of a few hours. The LLBL also provides the "voltage source" in this scenario (*cf.* Eastman *et al.*, 1976; Lundin *et al.*, 1995).

Attempts to verify, with statistical methods, that the GSE v_Y component (in the spin plane) of the H^+ and He^{++} bulk flows does have the proper sign in the region of inward flow, immediately adjacent to the lobes, have, however, met with mixed results. The probable reason for that is at least twofold. For one, it is difficult to obtain a measure of distance across the boundary between the lobe and the central plasma sheet, one that is independent of the flow measurements themselves. Using the local ratio between total ion gyrational energy density and the magnetic field pressure (the ion beta) has, for instance, proved inadequate. For another, the fairly low drift speed, typically a few tens of km s^{-1}, although sufficient to cause a significant deflection of tailward streams of cold O^+ ions (Orsini *et al.*, 1990), is much smaller than the mean gyration velocity of the H^+ and He^{++} ions (hundreds of km s^{-1}). As a result, the comparison of ion fluxes in

the positive and negative GSE y-directions, which are roughly parallel to the plasma sheet boundary, becomes sensitive to the ion density gradient near the boundary (a finite-gyroradii effect).

The only equipotential contours drawn in Figure 4 lie entirely on magnetic field lines that connect the northern and southern hemispheres of Earth, equatorward of the polar caps. There must be others, of course, and these need not have the same topology. It is conceivable, for instance, to have Points 2 and 3 in the lobe and polar cap, either with Point 1 still on a closed LLBL field line, or with Point 1 on a field line extending into the solar wind on the dawn flank. The latter is readily envisioned with a southward IMF, when the draping of the IMF against Earth's northward field is certain to create points of zero field along the flanks. In any case, an accurate mapping of electric potential must also account for finite potential differences along the magnetic field, and, especially with field lines extending far downtail, it must take into consideration the finite propagation time of changing potentials. The last point has bearing on the following discussion.

5. On the Earthward Flows of Solar Origin Plasma

The "classical" image of solar wind entry has been that it takes place at high latitude, across the tail lobe magnetopause, and that the solar origin particles first encounter the plasma sheet at some considerable distance downtail, of the order of 100 R_E, near a tail field "neutral line" (*e.g.* Cowley, 1980, and references therein). In that scenario the near-Earth plasma sheet must be populated via earthward (and sunward) flows, including jetting of plasma along the magnetic field (*e.g.* Speiser, 1965). Numerous reports of rapid (often in excess of 1000 km s^{-1}) earthward ion flows, many based on data from ISEE particle detectors (*e.g.* DeCoster and Frank, 1979; Lyons and Speiser, 1982; Eastman *et al.*, 1985; Hones *et al.*, 1986), may thus appear to validate this concept (*e.g.* Hones *et al.*, 1986), or at least to validate the notion that the near-Earth plasma sheet, to a large extent, is populated from more distant parts of the tail (*e.g.* Eastman *et al.*, 1985). This prospect was noted in Paper I, but no further analysis was attempted. This section is intended to remedy that omission by outlining a possible alternative interpretation of the earthward ion flows.

The basis for a different interpretation is twofold, including both general considerations of substorm dynamics and specific aspects of the ion flows themselves. For the general part, see Figure 5.

Panel a depicts the typical situation of plasma sheet thinning, or plasma "dropout", at the ISEE-1 in the early stage of a substorm (*e.g.* Hones *et al.*, 1986). This phenomenon was first recognized and diagnosed by Hones *et al.* (1971, and references therein) in electron data obtained simultaneously by two Vela spacecraft at 18 R_E. They noted that it involves a net loss of plasma and that the particle

pressure, as manifested by 0.1- to 18-keV electrons, drops throughout the plasma sheet latitudinal extent, at least in a region near local midnight, with the possible exception of the midplane, or "neutral sheet", whose position could not be determined with very good precision from the available data. Based in part on the sheer volume of their data, they concluded, however, that the plasma pressure in the midplane does not increase, but either remains about constant or drops there as well.

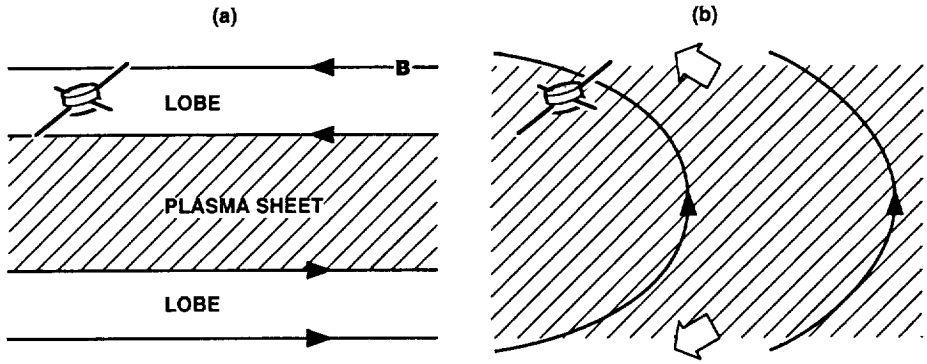

Figure 5. (a) Plasma sheet (cross hatched area) in a state of thinning due to increased earthward and sunward convection (to the left), leaving observing spacecraft in tail lobe. Direction of tail lobe magnetic field **B** indicated by thin lines with solid arrow heads. (b) Plasma sheet engulfing spacecraft again by expanding (open arrows) along magnetic field lines that are becoming increasingly dipole-like.

Panel b depicts the likely consequence if the plasma pressure does indeed drop in the tail midplane. Since the magnetic and particle pressures are normally in diamagnetic balance through the thickness of the tail (*e.g.* Fairfield *et al.*, 1981), a reduction of the particle pressure in the midplane, where it has its maximum, allows the tail magnetic field to reduce its internal energy by increasing its closure through the plasma sheet, that is to "dipolarize". This provides access, along magnetic field lines, of particles from the midplane to regions of lower plasma density, probably including adjacent parts of the lobes, as indicated, which, in turn, leads to further particle pressure reduction in the midplane, offset only by possible betatron acceleration associated with the locally increasing magnetic field strength B. Since the increase in perpendicular particle pressure due to increasing B is at most proportional to B (via the first adiabatic invariant), while the magnetic pressure is proportional to B^2, the field "dipolarization" effect must prevail, however.

In this scenario, the plasma sheet "recovery" at the ISEE-1, typically within less than 2 hours of the start of thinning (examples to follow), is not due to the

sudden arrival of new plasma from an external source, but merely to a redistribution of the pre-existing plasma sheet. The first ions to arrive are those with the shortest time-of-flight from some point within the downtail plasma sheet, which typically means ions with an earthward field-aligned velocity, that is earthward "jetting" ions, from the upper end of the ion energy distribution. These are subsequently joined by ions with decreasing earthward velocity, that is ions with increasing pitch angle and decreasing energy, eventually including ions that have mirrored closer to Earth and are returning tailward. In other words, the initial ion beam will appear to "evolve" into a typical isotropic plasma sheet population, more or less, which is qualitatively consistent with reported observations (*e.g.* Eastman *et al.*, 1985). The time scale of this evolution must depend on the location of the ISEE-1 in relation to the downtail point of origin of the ions, which may vary from event to event, and on the distance from Earth, but considering the time-of-flight of H^+ ions with energies between, say, 100 eV and 30 keV over distances of a few tens of R_E, it may well be of the order of 10 minutes. Such a number is also suggested by the observations (see for instance Figure 9 in Eastman *et al.*, 1985).

In its most literal interpretation, this scenario implies that the earthward jetting of ions does not occur at the initial thinning of the plasma sheet, only at the time of recovery, even though the lobe boundary of the plasma sheet can be said to "sweep across" the ISEE-1 in both cases. A survey of the "total ion" data from the composition experiment (the data with maximum time resolution) has revealed that this kind of asymmetry is indeed common, provided the substorm activity, as measured by the AE index, remains at a moderate level. As an example, Figure 6 shows four events of "moderate" plasma sheet thinning and recovery in a 12-hour period, while the ISEE-1 travels from $R = 16.5$ to $R = 21.5$ R_E at about 0200 local time. In all four events the maximum bulk flow speed (5:th panel down) occurs about the time of recovery of the number density (top panel) and perpendicular particle pressure (4:th panel; dashed line), and the flow direction is indeed sunward in each case, that is earthward (bottom panel; dashed line). The 1-minute AE remains below 300 nT through this period, except for a few minutes before 0600 UT, when it reaches about 700 nT (Kamei and Maeda, 1982). The 1-hour average IMF (from the IMP-8; see Couzens and King, 1986) remains southward, with B_Z about -3 nT to -2 nT, except for 0800-0900 UT, when $B_Z = +0.55$ nT.

This asymmetry disappears with increasing activity, and earthward ion flows begin to show up during plasma sheet thinning, as well. A reasonable explanation for this is that the process in Figure 5 moves tailward (see below) and that, during times of continued strong equatorward and earthward convection, the plasma sheet may thin again at the ISEE-1, while it is still recovering some distance further downtail and emitting earthward jets of ions, but this cannot be verified with the present data alone. However, there is another aspect of the observed earthward ion flows that can best be understood in terms of ions leaving the

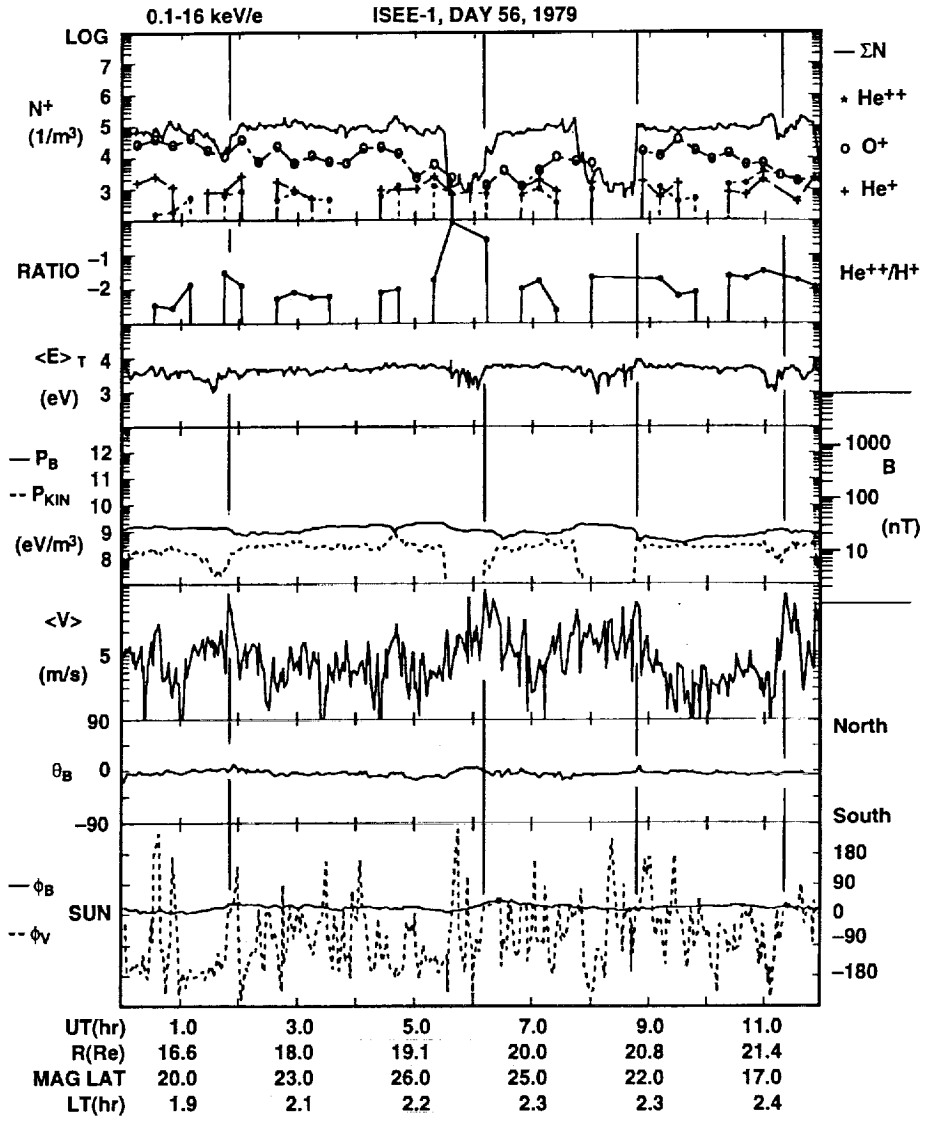

Figure 6. From top to bottom: number densities of "total ions" (assuming all H^+; solid line) and three mass resolved ions (symbols on the right); He^{++}/H^+ density ratio; thermal energy (bulk flow energy subtracted) of "total ions"; perpendicular pressures (in energy units) of magnetic field (solid line) and "total ions" (dashed line); bulk flow speed of "total ions"; direction angle of magnetic field above and below solar ecliptic plane; direction angles in solar ecliptic plane of magnetic field (solid line) and "total ion" bulk flow (dashed line).

plasma sheet, as opposed to ions entering from an external source. That aspect is the usually modest flux intensity, as illustrated in Figure 7.

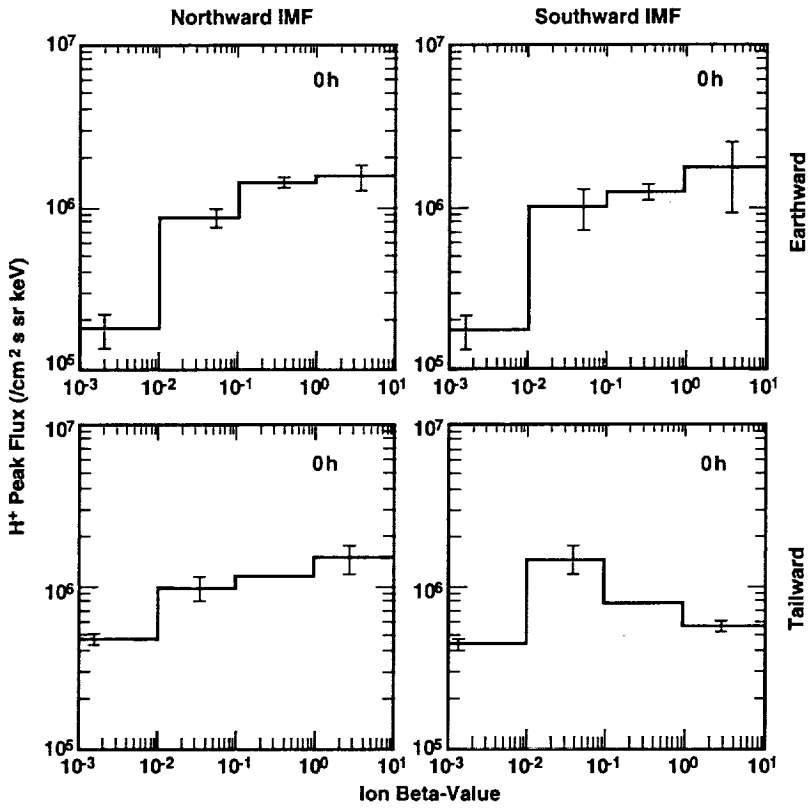

Figure 7. Averages of peak differential H^+ flux (peak flux per each energy-spin-angle cycle with mass analyzer set for M/Q = 1) in (top) the earthward direction (earthward half of 360°) and (bottom) tailward direction (tailward half), sorted by measured ion beta (adding partial pressures of the four principal ions; see text) and by direction of concurrent hourly IMF ("0 h" indicates no time shift). Extreme left and right bins in beta extend beyond scale. Samplings include all energies between 10 eV and 18 keV here, but are limited to those instrument cycles that cover all pitch angles (error bars again show ± 1σ of mean, if > 5%, and are placed at average beta in each bin).

This figure is tailored to the fact that the earthward field-aligned ion flows must occur in regions of low ion beta, whether they form a spatial outer boundary on the plasma sheet or, as argued here, constitute a time-of-flight effect. This is because, by definition, they locally dominate the ion flux and yet have little gyrational energy themselves. The beta used here is derived from the sum of partial perpendicular pressures of H^+, He^{++}, He^+, and O^+ ions, and the data are from within 10 R_E on either side of local midnight (*cf.* Lennartsson, 1994). Based on the distribution over beta of H^+ bulk flow speeds along the tail axis (see Figure 4 in Lennartsson, 1994), the strongly collimated earthward ion flows occur mostly at beta < 0.1. As Figure 7 suggests, the earthward flux intensities there are typi-

(4) Although collimated and fast (of order 1000 km s^{-1}) earthward "jets" of ions are often observed near the lobe boundaries of the plasma sheet, in a region of low ion beta, as might be expected with a downtail reconnection site, the typical flux per solid angle of these is, at most, comparable to the isotropic flux in the central plasma sheet (Figure 7).

Figure 5 is likewise an attempt to explain this last aspect, by conjecturing the effects of superimposing a dawn-dusk directed electric field of solar wind origin, when the IMF turns southward, on the "internally generated" field in Figure 4. In a geometrical sense, Figure 5 depicts what might be considered "reconnection", but that term has the connotation of a magnetic field being "carried along" by the plasma. The physical process envisioned here can best be described as a local "diamagnetic breakdown" of the plasma sheet, one where part of the tail lobe magnetic field intrudes into the central plasma sheet particle population. Such a process does have several attractive implications, some of which tie in with previous results:

(a) If the field intrusion is sufficiently rapid, that is rapid compared to gyrocenter gradient-*B* drift across the field, but still slow compared to the gyration period of H^+ ions (6.6 sec in a 10 nT field), the associated betatron acceleration, perhaps combined with pitch-angle scattering, will cause a rapid heating of the dominant ion component over a wide range of initial energies (final gyration energy of each ion proportional to its initial value, to the extent the first invariant is preserved). This ties in with the substorm-induced plasma sheet heating in general (*e.g.* Figure 1) and may help explain, in particular, the observations by Huang *et al.* (1992) of "nonadiabatic" (in a thermodynamic sense) heating of the central plasma sheet coincident with partial dipolarization of the magnetic field.

(b) If the rise time of the magnetic field strength *B* is longer than both the H^+ and He^{++} gyration periods (the latter only twice as long), it would explain why those two species tend to maintain nearly equal energy per nucleon (see Figure 1 and Point (4) in Section 2). Since the gyration period of electrons is then well within the requirement for preserving their first invariant, it would also explain why the plasma sheet electron temperature tends to be proportional to (but lower than) that of the positive ion component (*e.g.* Figure 9 in Baumjohann *et al.*, 1989). If the rise time of *B* is limited on the upper end by the gyration period of O^+ ions (almost 2 min in a 10 nT field), it would help explain why that terrestrial component is not heated during substorms (Figure 1, right panel), although the admixture of new O^+ ions probably plays a role, as well.

(c) If this magnetic field intrusion is most likely to occur in the vicinity of local midnight, where substorms are often initiated, it would help explain why the He^{++} and H^+ ions have a temperature maximum there (see Figure 12b in Lennartsson and Shelley, 1986, and adjoining text).

A crucial part of this scenario is the occurrence, in the earliest phase of substorms (growth phase), of near-Earth plasma sheet thinning, that is plasma

cally comparable to or smaller than the flux in the central plasma sheet, at beta > 0.1, as would be expected if the ion jets were composed of ions escaping from the central plasma sheet, perhaps at times occupying a smaller solid angle than even the instrument field of view. In contrast, if the ion jets were to supply the central plasma sheet from an external ion source, by being scattered in angle and energy, then one would expect these to be much more intense to start with (which is indeed the case with tailward flowing O^+ ions, as shown by Figure 2 in Lennartsson, 1995). Besides, these jets are part of the substorm process, and that process does reduce the number of solar origin ions in the plasma sheet, as already demonstrated (Figure 2).

It should be mentioned that the flux averages at beta < 0.1 in the top panels of Figure 7 remain essentially the same, within statistical error bars, if the data are strictly limited to samplings with the earthward H^+ bulk speed > 300 km s^{-1}. Also, the reduced tailward flux at beta > 1 in the bottom right panel may be a sampling bias, since the requirement of full pitch-angle coverage strongly limits the data selection there (*cf.* Section 1.1).

6. Concluding Remarks

There are several aspects of the ISEE ion composition data that cast doubts on the "classical" two-dimensional image of solar wind entry, the one where magnetosheath plasma from above Earth's magnetic poles is being forced toward a distant reconnection site in the magnetotail midplane by a dawn-dusk directed electric field imposed from the solar wind. Special weight has previously been placed on three of these aspects (in Paper I):

(1) When the H^+ and He^{++} ions are at their highest concentration in the near-Earth plasma sheet, they have a mean energy per nucleon that approximates their typical bulk flow energy in the solar wind (Figure 1), thus showing no evidence of substantial acceleration at a distant tail reconnection site.

(2) The total number of plasma sheet H^+ and He^{++} ions peaks during extended periods of geomagnetic quiescence (Figure 2), when the IMF remains northward and, hence, the solar wind electric field has a dusk-to-dawn direction, opposite that of the tail electric field required for reconnection.

(3) At times, a relatively dense (of order 1 cm^{-3}) and cool (about 1 keV/nucleon) population of H^+ and He^{++} ions with "solar wind-like" composition (a few per cent He^{++}) can be observed flowing slowly tailward (at about 100 km s^{-1}) near the lobe boundaries of the near-Earth plasma sheet (Figure 3).

Figure 4 is an attempt to explain these three aspects of the ISEE data by invoking electric potentials that allow a favorable three-dimensional tail plasma flow, one that is at least partially independent of the solar wind electric field.

This article adds a fourth aspect to this list:

(4) Although collimated and fast (of order 1000 km s^{-1}) earthward "jets" of ions are often observed near the lobe boundaries of the plasma sheet, in a region of low ion beta, as might be expected with a downtail reconnection site, the typical flux per solid angle of these is, at most, comparable to the isotropic flux in the central plasma sheet (Figure 7).

Figure 5 is likewise an attempt to explain this last aspect, by conjecturing the effects of superimposing a dawn-dusk directed electric field of solar wind origin, when the IMF turns southward, on the "internally generated" field in Figure 4. In a geometrical sense, Figure 5 depicts what might be considered "reconnection", but that term has the connotation of a magnetic field being "carried along" by the plasma. The physical process envisioned here can best be described as a local "diamagnetic breakdown" of the plasma sheet, one where part of the tail lobe magnetic field intrudes into the central plasma sheet particle population. Such a process does have several attractive implications, some of which tie in with previous results:

(a) If the field intrusion is sufficiently rapid, that is rapid compared to gyrocenter gradient-*B* drift across the field, but still slow compared to the gyration period of H^+ ions (6.6 sec in a 10 nT field), the associated betatron acceleration, perhaps combined with pitch-angle scattering, will cause a rapid heating of the dominant ion component over a wide range of initial energies (final gyration energy of each ion proportional to its initial value, to the extent the first invariant is preserved). This ties in with the substorm-induced plasma sheet heating in general (*e.g.* Figure 1) and may help explain, in particular, the observations by Huang *et al.* (1992) of "nonadiabatic" (in a thermodynamic sense) heating of the central plasma sheet coincident with partial dipolarization of the magnetic field.

(b) If the rise time of the magnetic field strength *B* is longer than both the H^+ and He^{++} gyration periods (the latter only twice as long), it would explain why those two species tend to maintain nearly equal energy per nucleon (see Figure 1 and Point (4) in Section 2). Since the gyration period of electrons is then well within the requirement for preserving their first invariant, it would also explain why the plasma sheet electron temperature tends to be proportional to (but lower than) that of the positive ion component (*e.g.* Figure 9 in Baumjohann *et al.*, 1989). If the rise time of *B* is limited on the upper end by the gyration period of O^+ ions (almost 2 min in a 10 nT field), it would help explain why that terrestrial component is not heated during substorms (Figure 1, right panel), although the admixture of new O^+ ions probably plays a role, as well.

(c) If this magnetic field intrusion is most likely to occur in the vicinity of local midnight, where substorms are often initiated, it would help explain why the He^{++} and H^+ ions have a temperature maximum there (see Figure 12b in Lennartsson and Shelley, 1986, and adjoining text).

A crucial part of this scenario is the occurrence, in the earliest phase of substorms (growth phase), of near-Earth plasma sheet thinning, that is plasma

depletion. Although that phenomenon is rather well established empirically (Hones *et al.*, 1971), it is worthwhile to briefly speculate about its possible cause:

Being that a newly southward IMF is going to affect the magnetopause flanks near dawn and dusk before it is transported downtail by the solar wind (in the magnetosheath), it seems reasonable that the near-Earth plasma sheet, as well as the dawn and dusk sectors of the auroral ovals, will experience the associated dawn-dusk electric field before the more distant portions of the plasma sheet do so, assuming there is good electric conduction along geomagnetic field lines threading the outer edge of the LLBL. The electric connection ought to be ensured, it seems, by the cancellation of the IMF at some point along the oppositely directed geomagnetic field line. If true, this implies that the near-Earth plasma sheet undergoes increased equatorward and sunward convection, of the kind normally associated with a dawn-dusk electric field (*e.g.* Hultqvist *et al.*, 1981), before there is increased inflow of plasma from further down the tail. This may well generate a sufficient divergence in the plasma flow to account for the thinning, including a drop in the plasma pressure in the midplane.

Furthermore, it is also reasonable that the thinning will progress tailward, either because the southward IMF is transported in that direction along the flanks, or because the dawn-dusk electric field already applied between the dawn and dusk sectors of the auroral ovals near Earth propagates outward along adjacent geomagnetic field lines that lead downtail, or by a combination of the two effects. Although the Alfvén velocity in the high-latitude plasma sheet (for example 1200 km s^{-1} with 0.3 cm^{-3} H^+ ions in a 30 nT field, or 11 R_E per min) is likely to be larger than the solar wind velocity along the flanks (a few hundred km s^{-1}), the near-Earth electric field has to reach the proper tail magnetic field lines first, so it is not obvious which effect may dominate.

This last excursion from actual data may serve as a reminder that the tail flanks, and in particular the LLBL, play a fundamental role in the above interpretation of ISEE data on solar origin ions. It is envisioned here that the LLBL probably is the "site of plasma, momentum and energy transfer" from the solar wind that it once was foreshown to be by Eastman *et al.* (1976). Although there has yet to be a consensus on the physics behind this boundary layer, speculating on that subject goes beyond the scope of this article.

Acknowledgments

This work was supported by NASA under grant NAGW-4177.

References

Balsiger, H., Eberhardt, P., Geiss, J., and Young, D.T.: 1980, 'Magnetic storm injection of 0.9- to 16-keV/*e* solar and terrestrial ions into the high altitude magnetosphere', *J. Geophys. Res.* **85**, 1645.

Baumjohann, W., Paschmann, G., and Cattell, C.A.: 1989, 'Average plasma properties in the central plasma sheet', *J. Geophys. Res.* **94**, 6597.

Collin, H.L., Peterson, W.K., Drake, J.F., and Yau, A.W.: 1988, 'The helium components of energetic terrestrial ion upflows: their occurrence, morphology, and intensity', *J. Geophys. Res.* **93**, 7558.

Couzens, D.A., and King, J.H.: 1986, *Interplanetary medium data book, supplement 3, 1977-1985*, Rep. NSSDC/WDC-A-R&S 86-04, NASA Goddard Space Flight Cent., Greenbelt, Md.

Cowley, S.W.H.: 1980, 'Plasma populations in a simple open model magnetosphere', *Space Sci. Rev.* **26**, 217.

DeCoster, R.J., and Frank, L.A.: 1979, 'Observations pertaining to the dynamics of the plasma sheet', *J. Geophys. Res.* **84**, 5099.

Eastman, T.E., Hones, E.W., Jr., Bame, S.J., and Asbridge, J.R.: 1976, 'The magnetospheric boundary layer: Site of plasma, momentum and energy transfer from the magnetosheath into the magnetosphere', *Geophys. Res. Lett.* **3**, 685.

Eastman, T.E., Frank, L.A., and Huang, C.Y.: 1985, 'The boundary layers as the primary transport regions of the Earth's magnetotail', *J. Geophys. Res.* **90**, 9541.

Fairfield, D.H., and Ness, N.F.: 1970, 'Configuration of the geomagnetic tail during substorms', *J. Geophys. Res.* **75**, 7032.

Fairfield, D.H., Lepping, R.P., Hones, E. W., Jr., Bame, S.J., and Asbridge, J.R.: 1981, 'Simultaneous measurements of magnetotail dynamics by IMP spacecraft', *J. Geophys. Res.* **86**, 1396.

Feldman, W.C., Asbridge, J.R., Bame, S.J., and Gosling, J.T.: 1978, 'Long-term variations of slected solar wind properties: IMP 6, 7, and 8 results', *J. Geophys. Res.* **83**, 2177.

Fujimoto, M., Terasawa, T., and Mukai, T.: 1997, 'The cold-dense plasma sheet: A GEOTAIL perspective', *Space Sci. Rev.*, this issue.

Fuselier, S.A., Shelley, E.G., and Lennartsson, O.W.: 1997, 'Solar wind composition changes across the Earth's magnetopause', *J. Geophys. Res.* **102**, 275.

Ghielmetti, A.G., Johnson, R.G., Sharp, R.D., and Shelley, E.G.: 1978, 'The latitudinal, diurnal, and altitudinal distributions of upward flowing energetic ions of ionospheric origin', *Geophys. Res. Lett.* **5**, 59.

Hones, E.W., Jr., Asbridge, J.R., and Bame, S.J.: 1971, 'Time variations of the magnetotail plasma sheet at 18 R_E determined from concurrent observations by a pair of Vela satellites', *J. Geophys. Res.* **76**, 4402.

Hones, E.W., Jr., Fritz, T.A., Birn, J., Cooney, J., and Bame, S.J.: 1986, 'Detailed observations of the plasma sheet during a substorm on April 24, 1979', *J. Geophys. Res.* **91**, 6845.

Huang, C.Y., Frank, L.A., Rostoker, G., Fennell, J., and Mitchell, D.G.: 1992, 'Nonadiabatic heating of the central plasma sheet at substorm onset', *J. Geophys. Res.* **97**, 1481.

Hultqvist, B., Aparicio, B., Borg, H., Arnoldy, R., and Moore, T.E.: 1981, 'Decrease of keV electron and ion fluxes in the dayside magnetosphere during the early phase of magnetospheric disturbances', *Planet. Space Sci.* **29**, 107.

Kamei, T., and Maeda, H.: 1982, *Auroral electrojet indices (AE) for January-June 1979,* Data Book No. 5, World Data Center C2 for Geomagn., Kyoto Univ., Kyoto, Japan.

Lennartsson, W.: 1992, 'A scenario for solar wind penetration of Earth's magnetic tail based on ion composition data from the ISEE 1 spacecraft', *J. Geophys. Res.* **97**, 19221.

Lennartsson, O.W.: 1994, 'Tail lobe ion composition at energies of 0.1 to 16 keV/*e*: Evidence for mass-dependent density gradients', *J. Geophys. Res.* **99**, 2387.

Lennartsson, O.W.: 1995, 'Statistical investigation of IMF B_z effects on energetic (0.1- to 16-keV)

magnetospheric O^+ ions', *J. Geophys. Res.* **100**, 23621.
Lennartsson, W., and Shelley, E.G.: 1986, 'Survey of 0.1- to 16-keV/*e* plasma sheet ion composition', *J. Geophys. Res.* **91**, 3061.
Lundin, R., Yamauchi, M., Woch, J., and Marklund, G.: 1995, 'Boundary layer polarization and voltage in the 14 MLT region', *J. Geophys. Res.* **100**, 7587.
Lyons, L.R., and Speiser, T.W.: 1982, 'Evidence for current sheet acceleration in the geomagnetic tail', *J. Geophys. Res.* **87**, 2276.
Mitchell, D.G., Kutchko, F., Williams, D.J., Eastman, T.E., Frank, L.A., and Russell, C.T.: 1987, 'An extended study of the low-latitude boundary layer on the dawn and dusk flanks of the magnetosphere', *J. Geophys. Res.* **92**, 7394.
Orsini, S., Candidi, M., Stokholm, M., and Balsiger, H.: 1990, 'Injection of ionospheric ions into the plasma sheet', *J. Geophys. Res.* **95**, 7915.
Rosenbauer, H., Grünwaldt, H., Montgomery, M.D., Paschmann, G., and Sckopke, N.: 1975, 'Heos 2 plasma observations in the distant polar magnetosphere: The plasma mantle', *J. Geophys. Res.* **80**, 2723.
Russell, C.T.: 1978, 'The ISEE 1 and 2 fluxgate magnetometers', *IEEE Trans. Geosci. Electron.* **GE-16**, 239.
Sharp, R.D., Johnson, R.G., Lennartsson, W., Peterson, W.K., and Shelley, E.G.: 1983, 'Hot plasma composition results from the ISEE-1 spacecraft', in R.G. Johnson (ed.), *Energetic Ion Composition in the Earth's Magnetosphere*, TERRAPUB, Tokyo, Japan, 231.
Shelley, E.G., Johnson, R.G., and Sharp, R.D.: 1972, 'Satellite observations of energetic heavy ions during a geomagnetic storm', *J. Geophys. Res.* **77**, 6104.
Shelley, E.G., Sharp, R.D., Johnson, R.G., Geiss, J., Eberhardt, P., Balsiger, H., Haerendel, G., and Rosenbauer, H.: 1978, 'Plasma composition experiment on ISEE-A', *IEEE Trans. Geosci. Electron.* **GE-16**, 266.
Speiser, T.W.: 1965, 'Particle trajectories in model current sheets, 1. Analytical solutions', *J. Geophys. Res.* **70**, 4219.

Address for correspondence: O.W. Lennartsson, Lockheed Martin Missiles & Space, Advanced Technology Center, Org. H1-11, Building 252, 3251 Hanover Street, Palo Alto, CA 94304, USA
(e-mail: lenn@space.lockheed.com)

Appendix II

THEORETICAL IMPLICATIONS FOR MAGNETOPAUSE PROCESSES

by O.W. Lennartsson

Lockheed Martin Space Systems /Advanced Technology Center
Palo Alto, California

Excerpt from

Magnetospheric Plasma Sources and Losses

Final Report of the ISSI Study Project on
Source and Loss Processes

Edited by
B. Hultqvist, M Øieroset and G. Paschmann
International Space Science Institute, Bern, Switzerland
and R. Treumann
Max-Planck-Institute of Extraterrestrial Physics, Garching, Germany

Kluwer Academic Publishers
Dordrecht /Boston /London

(also in *Space Science Reviews, Vol. 88,* Nos. 1-2, 1999)

5.3.4. GRADIENT AND POLARISATION DRIFT ENTRY

Ion composition (Lennartsson, 1992, 1997) and other plasma observations (*e.g.*, Fujimoto *et al.*, 1997) have revealed that solar wind plasma gains access to Earth's plasma sheet, not only during periods of southward IMF orientation but also during times of northward IMF orientation. According to the traditional view, the magnetopause ought to be 'closed' under these circumstances. In fact, H^+ and He^{+2} ions, of apparent solar origin, reach the greatest densities (often exceeding $1\,cm^{-3}$ and $0.03\,cm^{-3}$, respectively) and the most 'solar wind-like' energies (which are of order $1-2\,keV$ per nucleon) during extended periods of geomagnetic quiescence, when the IMF remains strongly northward. At these times, the density of H^+ and He^{+2} ions is especially large in the dawn and dusk flanks of the plasma sheet (Lennartsson and Shelley, 1986, Fujimoto *et al.*, 1997), adjacent to the LLBL (*e.g.*, Eastman *et al.*, 1976, 1985b; Mitchell *et al.*, 1987). Because the LLBL contains a dense plasma of solar wind origin and reaches greatest thickness during northward IMF (Mitchell *et al.*, 1987), the LLBL is potentially a significant source of plasma for the plasma sheet. Once inside the LLBL, the solar wind plasma $\mathbf{E} \times \mathbf{B}$ drifts antisunward and probably into the plasma sheet and towards the tail centre (Lennartsson, 1992, 1997). The cross-tail drift may take the specific form illustrated in Figure 4 of Lennartsson (1997). The initial stage of the entry process, the mechanism by which magnetosheath plasma crosses the magnetopause, is however a more complex issue.

It is conceivable that magnetic reconnection plays an important role in supplying the LLBL with magnetosheath plasma even during times of northward IMF (*e.g.*, Fuselier *et al.*, 1995), but there are nonetheless other mechanisms that may deserve more attention than they have received so far. This section is intended to revisit briefly what is arguably the least explored of all proposed interactions between solar origin particles and Earth's magnetic field, namely gradient drift entry, of magnetosheath plasma along the tail flanks (Wentworth, 1965; Fejer, 1965; Cole, 1974; Olson and Pfitzer, 1984, 1985; Treumann and Baumjohann, 1988, and references therein). The objective is not to explain this mechanism but merely to place it 'on the table' for future study. It is henceforth referred to by the acronym GDE (Olson and Pfitzer, 1984). At the end of this section, polarisation electric fields will be considered as another possible drift entry mechanism.

Olson and Pfitzer (1984) considered individual suprathermal magnetosheath particle orbits near the magnetopause to show that $1-10\,keV$ magnetosheath protons are deflected off the magnetopause for most directions of incidence, but that there is a narrow 'entry cone' of allowed incidence directions within 25° of the geomagnetic equator. Positive ions enter on the dawnside and electrons enter on the duskside, as illustrated in the upper panels of Figure 5.13. Particles with the opposite charges are specularly reflected. If the colder particles are treated as frozen to the magnetosheath magnetic field lines, the model predicts that the flanks of the magnetosphere would be continuously populated solely by a small

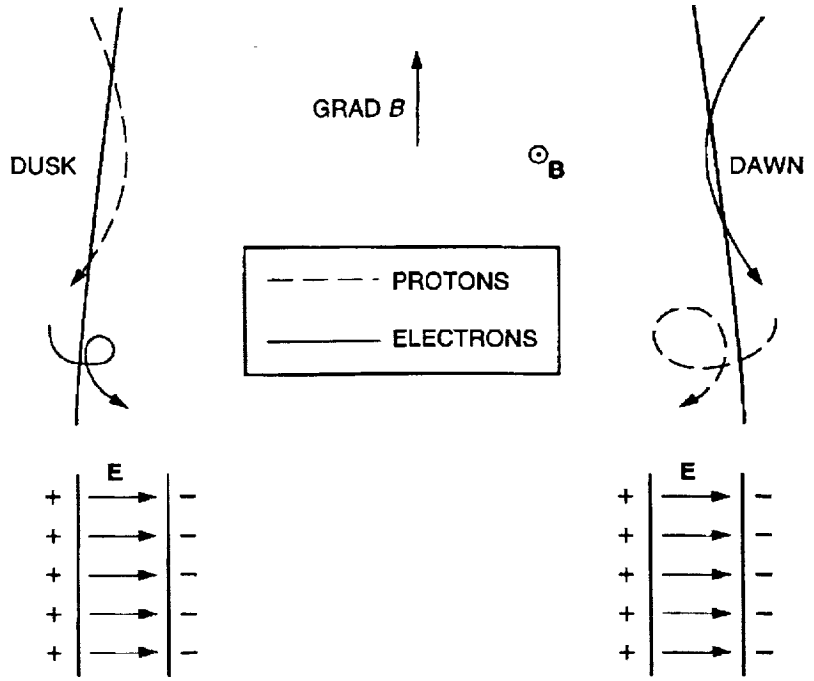

Figure 5.13. *Top*: Particle motion near the equatorial plane in a magnetotail magnetic field pointing out of the page with a gradient parallel to the magnetopause (adapted from Olson and Pfitzer, 1984; tail-flaring added). *Bottom*: Postulated boundary layer electric field.

fraction of the incident suprathermal magnetosheath plasma, primarily by protons which are substantially more energetic than the electrons. The curvature of the magnetopause may support the entry and contribute to dawn-dusk asymmetry.

Such particle drifts play an important role in the interaction of laboratory plasma beams with terrella dipole magnets, at least for protons. Cladis *et al.* (1964) considered the entry of an ionised hydrogen beam into the 'west' side of a magnetic dipole cavity. However, scaling laws suggest that such laboratory results would be more applicable to a beam of solar cosmic rays than solar wind particles.

Olson and Pfitzer (1985) proceeded to argue that all of the magnetosheath plasma striking the equatorial magnetopause directly enters the magnetosphere, thereby providing more than enough plasma to account for the observed flow of plasma down the magnetotail. However, Treumann and Baumjohann (1988) showed that no more than about 5% of the *energetic* magnetosheath plasma component may enter the LLBL by gradient drift. The main effect of this drift is to generate normal currents which locally distort the magnetopause.

The fundamental unresolved issue raised by application of a single-particle approach in the magnetospheric context is the disposal of electric charges that are

generated when protons and electrons diverge. As argued by Olson and Pfitzer (1985), charges may be redistributed via large-scale currents. They proposed that the entering particles continue to drift across the magnetotail plasma sheet, producing a current consistent with that observed. They argued that the build up of opposite charges just outside the magnetopause (due to the missing particles which have entered the magnetotail) induces a dusk-to-dawn return current across the high latitude magnetopause. Finally, they suggested that some built up charge is released as currents which flow down into the ionosphere in the observed region-1 Birkeland current sense.

If not stopped, the entering particles would simply gradient-curvature drift across the magnetotail, gaining energy from the normally dawn-to-dusk electric field within the plasma sheet. This would result in a distinct dawn-dusk asymmetry in H^+ and He^{+2} ion energies, which conflicts with observations indicating peak energies near the tail centre (Lennartsson and Shelley, 1986). Another possibility is that a polarisation electric field develops in the boundary layer, as indicated in the bottom part of Figure 5.13, which forces the plasma to drift antisunward. The thickness of the LLBL is not related in a simple manner to either the inward drift speed or the particle gyroradii, because the sunward gradient in the tail magnetic field is associated with a flaring of the magnetopause, which implies that different magnetosheath particles can enter at different distances from the tail axis.

To date, the self-consistent effects of the induced electric field in such a boundary layer have not been considered. Pure gradient-B drift must progress at a rather modest speed near the dawn and dusk magnetopause, on the order of ~ 0.1 km per minute per eV of particle energy (Treumann and Baumjohann, 1988). Charge separation effects become significant on Debye length spatial scales, on the order of tens of metres in this region of space (where electron densities are several cm^{-3} or more, and thermal energies are at most a few hundred eV), which is small even compared to electron gyroradii (which are $\sim$ 2 km in a 20 nT field for particles with energies of 100 eV). Hence, pure ∇B-drift is virtually impossible and interparticle electric forces must become significant within a single gyration of the entering particles, be they protons or electrons.

Two major predictions emerge if entry were to occur solely by the gradient-drift mechanism. Gradient-drift entry predicts (1), a steady antisunward flowing plasma in the boundary layer, regardless of IMF orientation, and (2), an increase in the total flux of plasma flowing tailward on closed magnetospheric magnetic field lines with downstream distance. However, the available tail observations do not necessarily confirm the presence of a dense region of antisunward flowing plasma on closed magnetic field lines. While the plasma sheet velocity definitely increases with downstream distance (Zwickl *et al.*, 1984; Paterson and Frank, 1994), the density may (Zwickl *et al.*, 1984) or may not (Paterson and Frank, 1994). The increase, if any, in antisunward flux is generally considered to occur on southward, or open, magnetic field lines produced by reconnection in the mag-

netotail plasma sheet (Slavin *et al.*, 1985). Whether the contribution from gradient drift is significant remains to be seen. It may be necessary to use hybrid or particle simulations in order to account for gradient drift and space charge effects.

By comparison with gradient-drift entry, another potential drift entry mechanism, caused by electric polarisation, has received even less attention. The difference in the electron and ion gyroradii may cause a charge separation electric field at the magnetopause (see bottom of Figure 5.13). Temporal variations of this polarisation field will generate polarisation drifts of the ions normal to the magnetopause. If one postulates that this field varies on the time scale of the ion gyro frequency, with an amplitude of a few $mV\,m^{-1}$, an ion drift of order of a few $km\,s^{-1}$ would result. Such drifts would be significant for particle entry.

5.3.5. GRADIENT DRIFT EXIT

Thermal and energetic particles of magnetospheric origin are commonly observed within a narrow magnetosheath layer at and immediately outside all regions of the magnetopause (Meng and Anderson, 1970; Hones *et al.*, 1972). The extrapolated energy flux carried by electrons with energies in excess of 10 keV ranges from 3×10^8 during quiet times to 3×10^{11} W during disturbed times (Baker and Stone, 1977). Ions with energies in excess of 50 keV carry a similar energy flux (Williams, 1979). We know that these particles are of magnetospheric origin because their composition (Sonnerup *et al.*, 1981; Peterson *et al.*, 1982) and spectra (Williams *et al.*, 1979) are similar to those for particles immediately inside the magnetosphere. The flux of energetic electrons is greatest outside the dawnside magnetopause, and the flux of energetic ions is greatest outside the duskside magnetopause (Meng *et al.*, 1981), consistent with the fact that the ions gradient and curvature drift westward, and the electrons eastward, to the points where their drift paths intersect the magnetopause. Spacecraft immediately inside the magnetopause can remotely sense a loss boundary from which ions do not return (Williams *et al.*, 1979). Moreover, the loss of electrons with 90° pitch angles from the pre-noon magnetopause is manifested by their absence from so-called 'butterfly' pitch angle distributions in the post-noon magnetosphere (West *et al.*, 1973). Similarly, the loss of ions from the post-noon magnetopause is manifested by their absence from butterfly pitch angle distributions in the pre-noon magnetosphere (Sibeck *et al.*, 1987c). Finally, flux levels in the magnetosheath increase with increasing geomagnetic activity (Frank and Van Allen, 1964; Meng and Anderson, 1970, 1975; West and Buck, 1976), consistent with the fact that flux levels within the magnetosphere itself increase with increasing activity.

While the above observations provide overwhelming evidence that the magnetosphere generally provides the main contribution to the energetic particle population found within the inner magnetosheath, the question of how the magnetospheric particles escape remains open. They are free to stream outward along

interconnected magnetosheath and magnetospheric magnetic field lines (Speiser *et al*, 1981) and observations of their anisotropies parallel or opposite to magnetosheath magnetic field orientations have often been taken as evidence for the presence of the tilted subsolar reconnection predicted by some models (*cf. e.g.*, Daly *et al.*, 1984).

Magnetic reconnection is not the only means by which magnetospheric particles may escape from the magnetosphere into the magnetosheath (*cf. e.g.*, Sibeck and McEntire, 1988). Energetic magnetospheric ions with energies of ~ 100 keV (and the very rare energetic electrons with energies of ~ 200 MeV) have gyroradii comparable to the ~ 800 km median thickness of the magnetopause current layer reported by Berchem and Russell (1982a). The orbits of particles with energies of this order simply pass across the magnetopause. With or without the presence of a finite magnetic field component normal to the magnetopause, the particles will be scattered in the current layer. Some precipitate into the ionosphere (Lyons *et al.*, 1987), but most probably stream away from the magnetosphere into the magnetosheath. In fact, the very same anisotropy observations used to confirm that ions escape from the magnetosphere along reconnected field lines are entirely consistent with escape via gradient-curvature drift (Sibeck *et al.* 1987b). The fact that the energetic ions are present outside the magnetopause for both northward and southward IMF conditions suggests that they are always escaping whether or not conditions favour reconnection (Sibeck *et al.*, 1987a,b).

5.4. Diffusion

5.4.1. INTRODUCTION

The focus of this section is on cross-field diffusive plasma entry and exit processes as possible mechanisms for cross-magnetopause plasma transfer. This includes micro, macro, and turbulent diffusion processes. Cross-field diffusion of cool sheath plasma into the LLBL may play a significant role in regions where or under conditions when magnetic reconnection is not operative or is not efficient. Such conditions may in particular be realised when the sheath magnetic field, which is the compressed interplanetary magnetic field, points northward.

The role of diffusion can, in principle, be deduced by observing the flow and field characteristics of the LLBL, together with the magnetic topology of the region, for example, from the observed spatial profiles of the LLBL. Sharp changes in the profiles may correspond to boundaries or discontinuities associated with reconnection (*cf. e.g.*, Gosling *et al.*, 1990; Song *et al.*, 1994). Smooth and gradual profiles may be indicative of diffusive plasma entry (*cf. e.g.*, Thorne and Tsurutani, 1991). The variation of the thickness of the LLBL along the magnetopause with increasing distance from the subsolar point also contains information on the magnetopause processes. A lack of increase of the thickness would be

Appendix III

RELATIVE ABUNDANCE OF SOLAR AND TERRESTRIAL IONS IN THE TAIL

by O.W. Lennartsson

Lockheed Martin Space Systems /Advanced Technology Center
Palo Alto, California

Excerpt from

Magnetospheric Plasma Sources and Losses

Final Report of the ISSI Study Project on
Source and Loss Processes

Edited by
B. Hultqvist, M Øieroset and G. Paschmann
International Space Science Institute, Bern, Switzerland
and R. Treumann
Max-Planck-Institute of Extraterrestrial Physics, Garching, Germany

Kluwer Academic Publishers
Dordrecht /Boston /London

(also in *Space Science Reviews, Vol. 88,* Nos. 1-2, 1999)

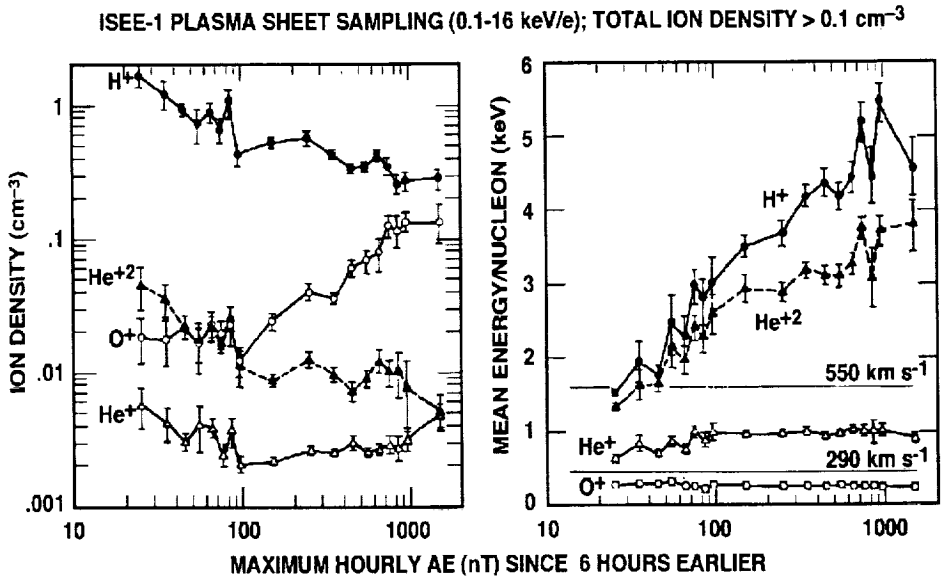

Figure 6.19. Central plasma sheet densities (left) and mean energies (right) of the four major ions, averaged over space and sorted according to the maximum level of auroral electrojet (AE) activity during the sampling and the preceding 6 hours. The thin horizontal lines in the right panel indicate the range of energy per nucleon that corresponds to the most common range of solar wind speeds. Error bars show the standard deviation (adapted from Lennartsson, 1992).

First we examine the observations in the near-Earth part of the tail and then in the distant tail. Finally we consider the use of observations of He^{+2} and of high charge states of carbon ($C^{\geq+5}$)and oxygen ($O^{\geq+6}$) to indicate a solar wind source.

Bulk Ion Sources in the Near Tail

The near-equatorial ISEE 1 spacecraft, with an apogee at $23\,R_E$, has provided a wealth of compositional information in the magnetotail beyond $10\,R_E$ for ions in the sub-keV to keV energy range (*e.g.*, Lennartsson and Shelley (1986) and references therein). The period of observation spanned the rising and maximum phases of solar cycle 21, from late 1977 to early 1982. Figure 6.19 summarises two years of measured densities and mean (thermal) energies of the four principal ionic components of the central plasma sheet in the context of geomagnetic activity. As evidenced by the presence of both He^{+2} and O^+, there are usually both solar and terrestrial ions present in significant numbers, although the relative mixture tends to vary with geomagnetic activity and solar cycle. Of course there is no direct way to distinguish the origin of H^+. But if it is assumed that the solar origin component in the plasma sheet retains the same He^{+2}/H^+ ratio as that in the solar wind (Lennartsson and Shelley, 1986), it follows that the solar component is dominat, by about two orders of magnitude, during extremely quiet geomagnetic

conditions. However, the terrestrial component (including the He^+) increases with increasing activity and may reach concentrations comparable to or greater than the solar component during extremely disturbed conditions, in part because the solar component decreases.

Defining 'intermediate' geomagnetic conditions by a maximum AE of 100 to 300 n, and assuming that all $H^+$is of solar origin, the ratio of terrestrial to solar wind ions is still low, typically 3% to 7%. If AE has been maintained at an average of 100 to 300 nT for at least a few of hours in sequence, this ratio is larger, about 8% to 20% (see Lennartsson and Shelley (1986) for details), at least in the energy range of these data (0.1 to 16 keV e^{-1}).

The basis for the assumption that the terrestrial part of the H^+ is much smaller than the solar part over most of the AE range is twofold: With the exception of the very highest AE ($\geq$ 1000 nT), the He^{+2}/H^+ ratio remains fairly constant even as the O^+ density increases almost tenfold, and the mean energies of both the H^+ and the He^{+2} ions increase with increasing AE, unlike the energies of O^+ and He^+ ions The reason why the observed average He^{+2}/H^+ ratio, 2%–3%, is lower than what is usually reported from the solar wind (3%–5%) may be, at least in part, that the penetration of solar ions through the magnetopause is mass dependent, discriminating against He^{+2} (Fuselier *et al.*, 1997).

Using the He^{+2}/H^+ ratio density ratio observed at low AE to represent the solar component that enters through the magnetopause, one obtains significantly different estimates of the relative source strengths from Figure 6.19. For example, at minimum AE ($\approx$ 10)one still estimates only a 2% ionospheric component; however, at intermediate activities (AE $\approx$ 200), the ratio increases to $\approx$ 40%. Thus the relative source strength estimates are very sensitive to the relative allocation of H^+, the dominant species except at very high activity levels.

Although the ion number densities are generally much lower in the tail lobes, and statistics are correspondingly more sparsely, it appears from the ISEE 1 data that the relative terrestrial contribution to the near-tail plasma is greater outside the plasma sheet proper (*e.g.*, Sharp *et al.*, (1981); Candidi *et al.*, (1982); Orsini *et al.*, (1990); Lennartsson, (1994)). In particular, Sharp *et al.* (1981) inferred that the central lobe plasmas primarily contain tailward directed, often strongly collimated, streams of terrestrial ions, mostly O^+, with low bulk energy ($<$ 1 keV). By comparing the O^+ streams observed in the lobes and the plasma sheet, Sharp *et al.* (1981) and Orsini *et al.* (1990) concluded that these streams are a significant, possibly dominant, source of the plasma sheet O^+ population as a whole, undergoing angular scattering and bulk heating inside the plasma sheet. Like the number density of O^+ ions in Figure 6.19 the frequency of occurrence of these streams seems to increase with increasing geomagnetic activity (*e.g.*, Sharp *et al.*, (1981)).

By further analysing the O^+ streams with a high-resolution positive-ion detector on the companion ISEE 2 spacecraft, Orsini *et al.* (1990) have demonstrated

that the stream alignment in the ecliptic (GSE x-y) plane (centre plane of their detector field of view), measured relative to the projected magnetic field direction in the same plane, is often consistent with 10 to 40 km s^{-1} $\mathbf{E} \times \mathbf{B}$ drift. This drift tends to be inward, toward local midnight, on the lobe sides of the plasma sheet and outward, toward the tail flanks, well inside the plasma sheet. These findings have potentially very significant implications for the entry of both terrestrial and solar ions into the plasma sheet, as argued by Lennartsson (1992; 1997).

Geomagnetic indices, such as AE, bring statistical order to the occurrence of O^+ ions in the plasma sheet, suggesting a specifically substorm-related origin of these ions. However, the response of the occurrence rate of the ions to changes in the solar wind conditions differs significantly from the response of the geomagnetic indices to these changes. The O^+ number and energy densities in the plasma sheet depend only marginally on the current or recent IMF B_z orientation (GSM coordinates). This is in stark contrast to the marked increase of the concurrent AE. On average, the O^+ energy density is only $\sim 60\%$ larger after a few hours of consistently southward B_z, as compared to the conditions following the same length period of consistently northward B_z. The corresponding increase in AE is by a factor of four or larger and is probably due in part, at least, to the lack of ground stations at the high latitudes of the contracted auroral oval during northward B_z (Lennartsson, 1995). These results seem to imply that the plasma sheet O^+ ions have a fairly steady source in the high-latitude ionosphere, perhaps mainly on the dayside, rather than an intermittent source only activated during substorms. This scenario is further supported by the fact that the tailward streams of O^+ ions have comparable intensities with both positive and negative IMF B_z (Lennartsson,1995; see also Figure 2.32).

Returning to Figure 6.19, it is thus important to note that the large average O^+ density at high AE is strongly biased by data taken during times of southward IMF (expanded auroral oval) and strong input of solar wind power to the ionospheric O^+ source. The location of stations used to measure the AE index is biased toward the expanded auroral oval and therefore toward activity associated with southward B_z. Thus, by correlating O^+ densities with AE only, one does not identify source enhancements that might be driven by strongly northward B_z.

As an alternative to the use of the AE index to correlate with the O^+ source, Lennartsson (1995) investigated the relationship between increased O^+ in the tail and high geomagnetic activity by examining the O^+ number and energy densities in the plasma sheet and the solar wind energy flux. He finds good correlation irrespective of the B_z polarity. It is clear from the observations that both sources contribute to the plasma in the near-Earth magnetotail. The solar wind dominates during quiet magnetospheric conditions; during disturbed intervals the ionosphere becomes relatively more important, probably dominating at the highest activity levels.